Physics of weak bosons

Pavel Staroba
Institute of Physics ASCR
06.10 2022

Outline

- First stage of investigation of weak interaction: identification of beta decay, continuous spectrum of electron in beta decay, neutrino hypothesis, first idea of intermediate bosons, further examples of weak processes, development of Fermi based theory of weak interaction, detection of antineutrino and neutrino, V-A effective field theory of weak interaction.
- Standard model of electroweak interaction: Glashow SU(2)xU(1) theory, Nambu, Goldstone, works of Brout, Englert and Higgs, Weinbergs's "Model of leptons", Veltman and t'Hooft proof of renormalisability, QCD, lagrangian of standard model
- Experimental confirmation of Weinberg's theory: discovery of weak currents
- Experimental confirmation of weak bosons W and Z: UA1 and UA2 at SPS
- Investigation of W and Z at e+ e- colliders: LEP, SLC
- Investigation of W and Z at Tevatron: CDF, D0
- Selected results of : ATLAS
- Conclusions

Early history of investigation of weak interaction

1896-1958

- 1896, Ernst Rutherford : identification of beta component in the radioactive rays emitted from uranium
- 1914, James Chadwick : energy spectrum of beta rays is continuous
- 1930, Wolfgang Pauli : postulation of neutrino hypothesis for the explanation of the continuous beta spectrum
- 1934, Enrico Fermi : formulation of the first field theory of beta decay – Fermi theory
- 1938, Oskar Klein : first theory of weak interaction with weak vector bosons.
- Forties and fifties: further information on the properties of weak interaction from weak decays of muon and strange hadrons, prediction and confirmation of parity violation, universality of Fermi theory
- 1958, Robert Marshak and George Sudarshan and by Feynman and Gell-Mann V – A theory

Standard model

1961-1973

- SU(2) x U(1) theory introducing weak neutral Z boson for the first time (Sheldon Glashow 1961, Abdus Salam and J.C. Ward 1964)
- 1961-1963, Jeffrey Goldstone, Abdus Salam, Steven Weinberg : Goldstone theorem
- 1964, F. Englert, R. Brout and Peter Higgs : BEH mechanism
- 1967, Steven Weinberg : SU(2) x U(1) theory of electroweak interaction with masses of weak bosons generated using BEH mechanism
- 1971-1972, Gerard 't Hooft and Martinus Veltman: rigorous proof of renormalizability of the massive Yang-Mills quantum fields theory with spontaneously broken gauge invariance
- 1973, David Gross, David Politzer, Frank Wilczek : QCD
- 1973, Steven Weinberg : Lagrangian of standard model including QCD and electroweak part

$$v = \frac{\mu}{\sqrt{\lambda}} = \frac{1}{\sqrt{G_F \sqrt{2}}} \doteq 246 \text{ GeV}$$

$$M_H = \lambda\, v$$

$$\theta_W = \tan^{-1}\left(\frac{g'}{g}\right)$$

$$M_W = \frac{g\, v}{2} = \frac{e\, v}{2\sin\theta_W}$$

$$M_Z = \frac{v}{2}\sqrt{g^2 + (g')^2} = \frac{e\nu}{2\sin\theta_W \cos\theta_W} = \frac{M_W}{\cos\theta_W}$$

$$e = g \sin(\theta_W)$$

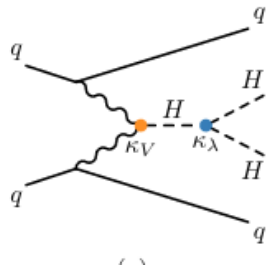

https://doi.org/10.1007/JHEP07(2020)108
http://www.nobelprize.org/nobel_prizes/physics/laureates/2013/advanced.html

Discovery of neutral currents
CERN 1973, Gargamelle

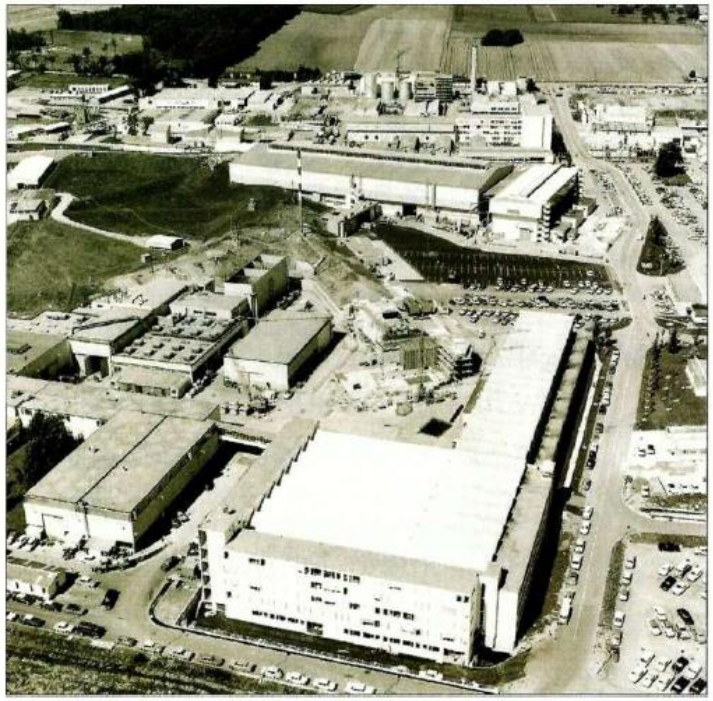

This 1967 aerial view of CERN shows (top left) the mound over the 28 GeV PS proton synchrotron with, pointing downwards and to the right, the beamline feeding the Gargamelle heavy-liquid bubble chamber, where neutral currents were discovered in 1973. In 1976 Gargamelle was laboriously reinstalled further away to work with the neutrino beams from CERN's new 450 GeV SPS proton synchrotron.

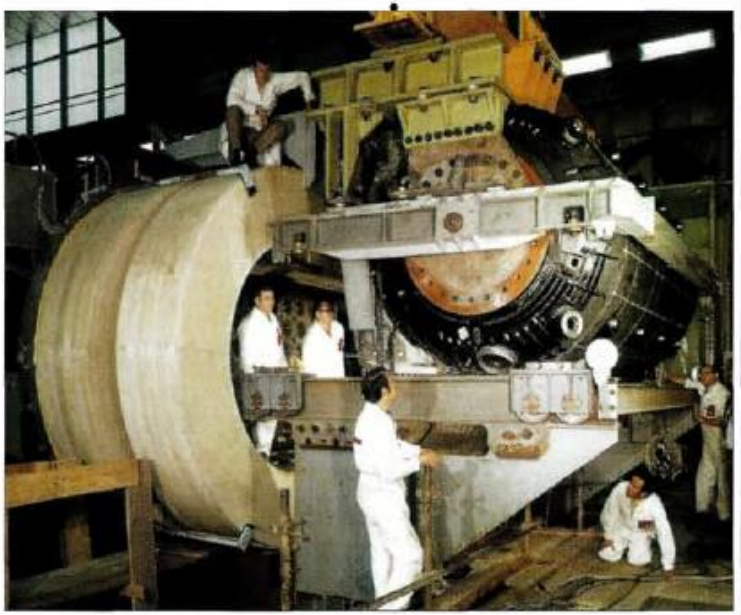

Fig. 1. The Gargamelle heavy-liquid bubble chamber, installed into the magnet coils, at CERN in 1970.

Table 1

	ν-exposure	$\bar{\nu}$-exposure
No. of neutral-current candidates	102	64
No. of charged-current candidates	428	148

CERN courier 1998 n. 8, 2004 n. 8

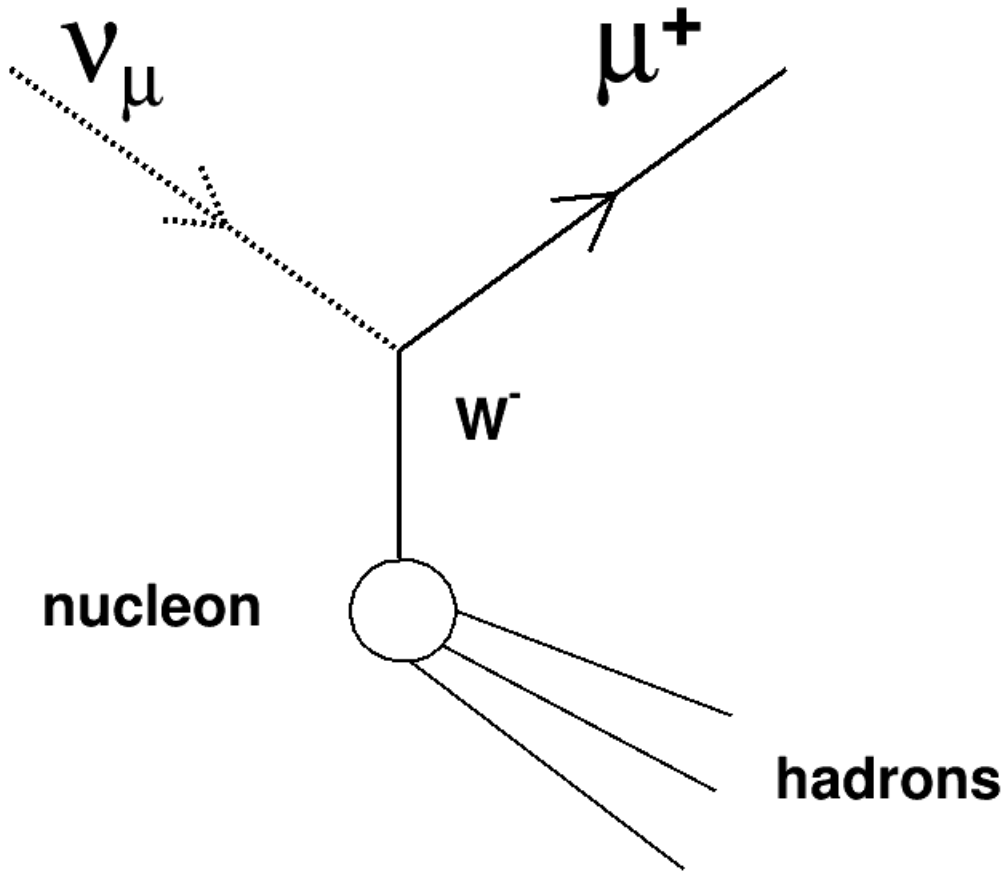
ν_μ
μ^+
W^-
nucleon
hadrons

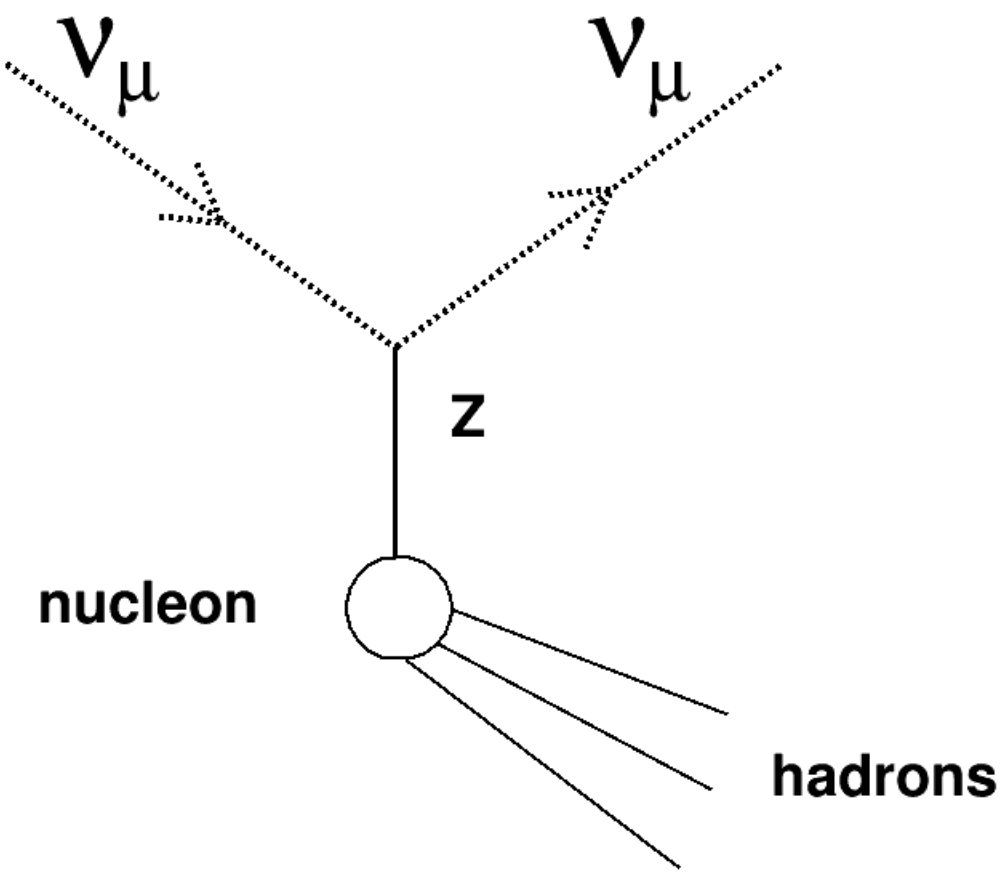
ν_μ
ν_μ
Z
nucleon
hadrons

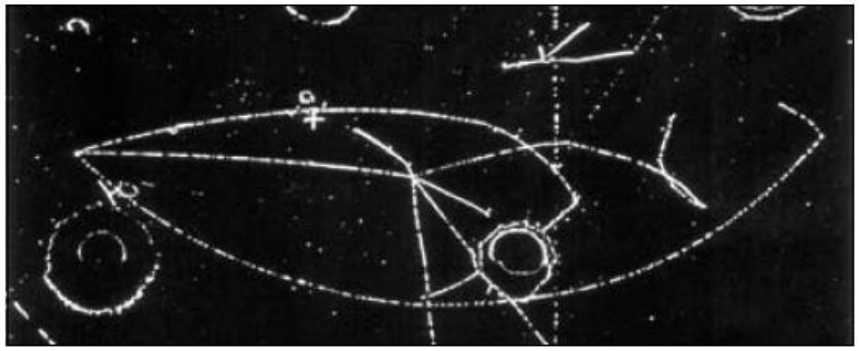

Fig. 1. A hadronic neutral current event, where the interaction of the neutrino from the left produces three secondary particles, all clearly identifiable as hadrons, as they interact with other nuclei in the liquid. There is no charged lepton.

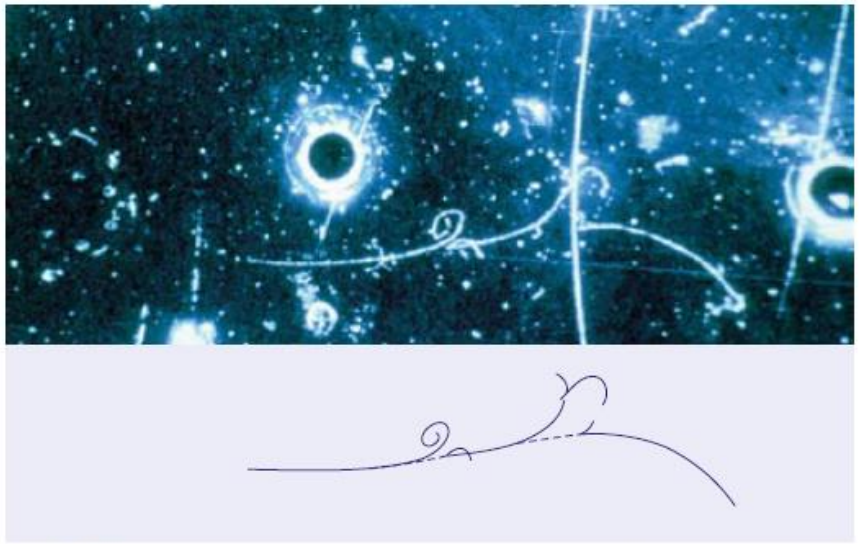

Fig. 2. The first leptonic neutral current event. An antineutrino coming from the left knocks an electron forwards, creating a characteristic shower of electron–positron pairs.

Discovery of neutral currents
CERN 1973, Gargamelle

Observation announced:
Bonn 1973
London 1974

Observation triggered huge activity both in experimental testing SM and calculations providing exact predictions

Nobel Prize in Physics 1979: Sheldon Lee Glashow, Abdus Salam and Steven Weinberg
"for their contribution to the theory of the unified weak and electromagnetic interactions between elementary particles, including, inter alia, the prediction of the weak neutral current".

CERN courier 2013 n. 7

Direct observation of W and Z
CERN SPS 1982-1991, UA1, UA2
540 – 630 GeV

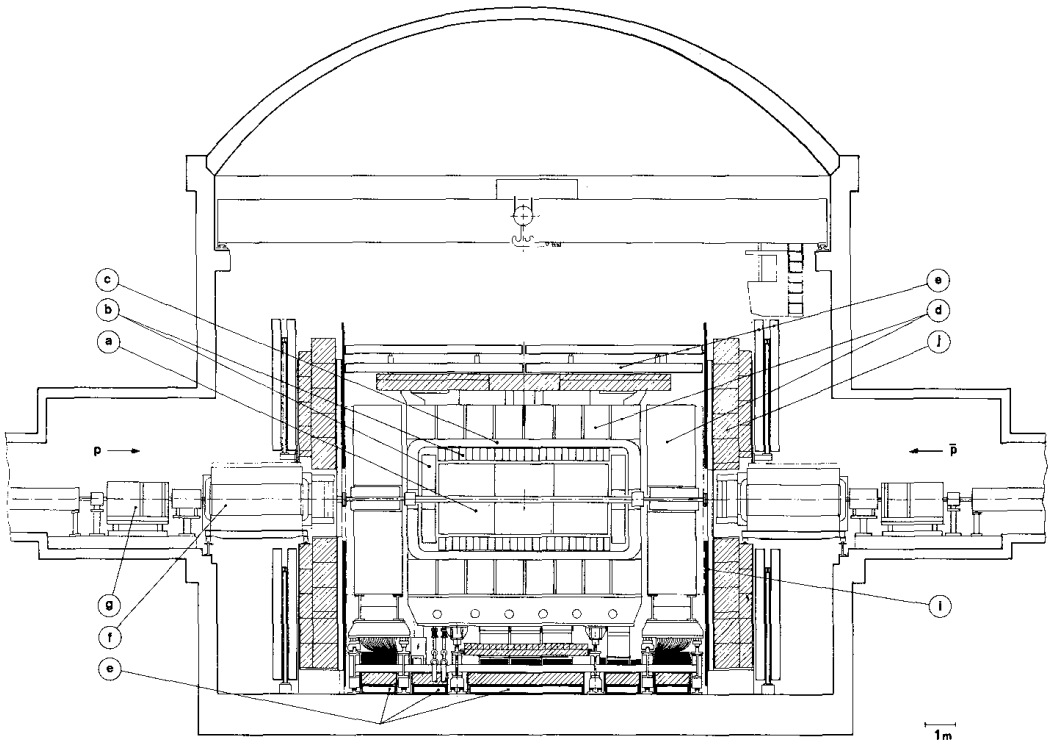

Fig. 2. A side view of the UA1 experiment at the time of the *W* and *Z* discovery 1982–1983. *a* The central detector. *b* The electromagnetic calorimeter (gondola, bouchon). *c* The coil, *d* The hadronic calorimeter (and the iron field return) (C's, I's). *e* The external muon chambers. *f* The forward calorimeters (Calcom). *g* The very forward calorimeters. *h* Instrumented magnetized iron side wall (added in 1984)

Z. Phys. 44, 15-61 (1989)

Schematic view of the creation

of the Drell-Yan Z^0 boson in the proton-proton interaction

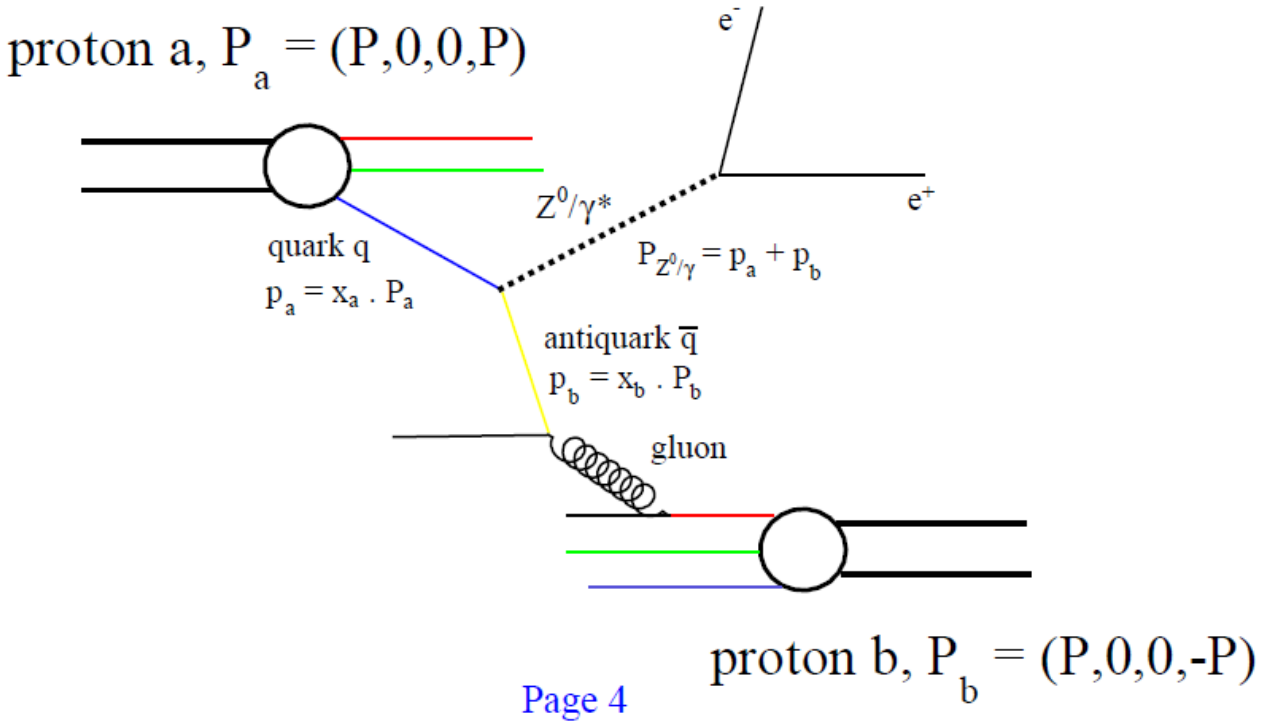

Page 4

Interactions of interest:

uD -> W+ and
Ud -> W-
uU -> Z
dD -> Z .

Decay channels used for detection

W+ -> e+ nu_e
W+ -> mu+ nu_mu
W- -> e- Nu_e
W- -> mu- Nu_mu

Z-> e+ e-
Z-> mu+ mu-

$$m_T = \sqrt{2.p_{T,e}.p_{T,\nu}.(1-\cos(\Phi_{e,\nu}))}$$

$\Phi_{e,\nu}$: difference of
azimuthal angles of e and ν

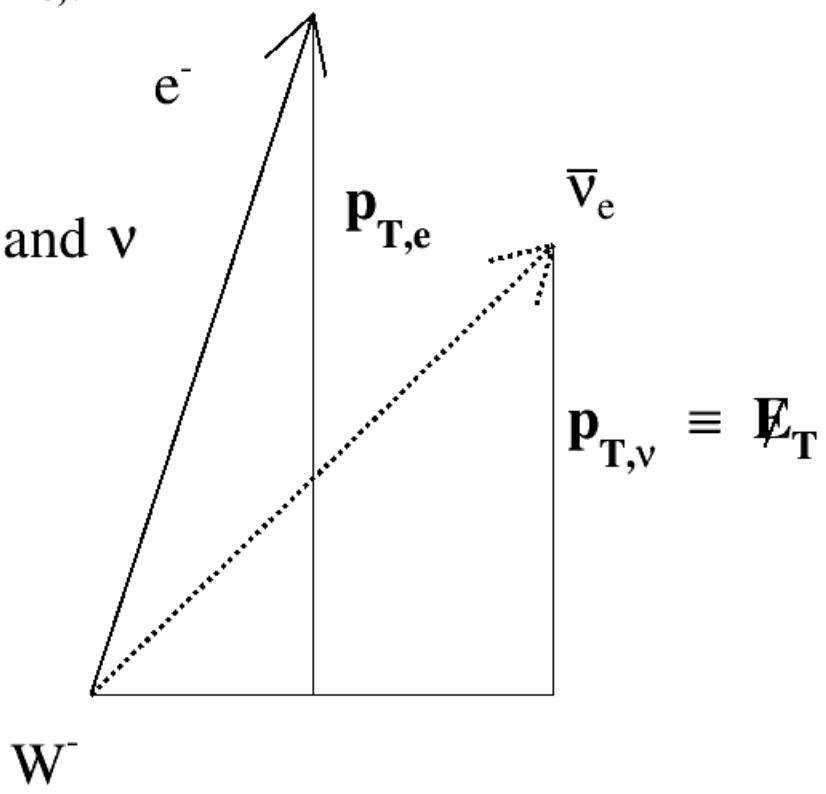

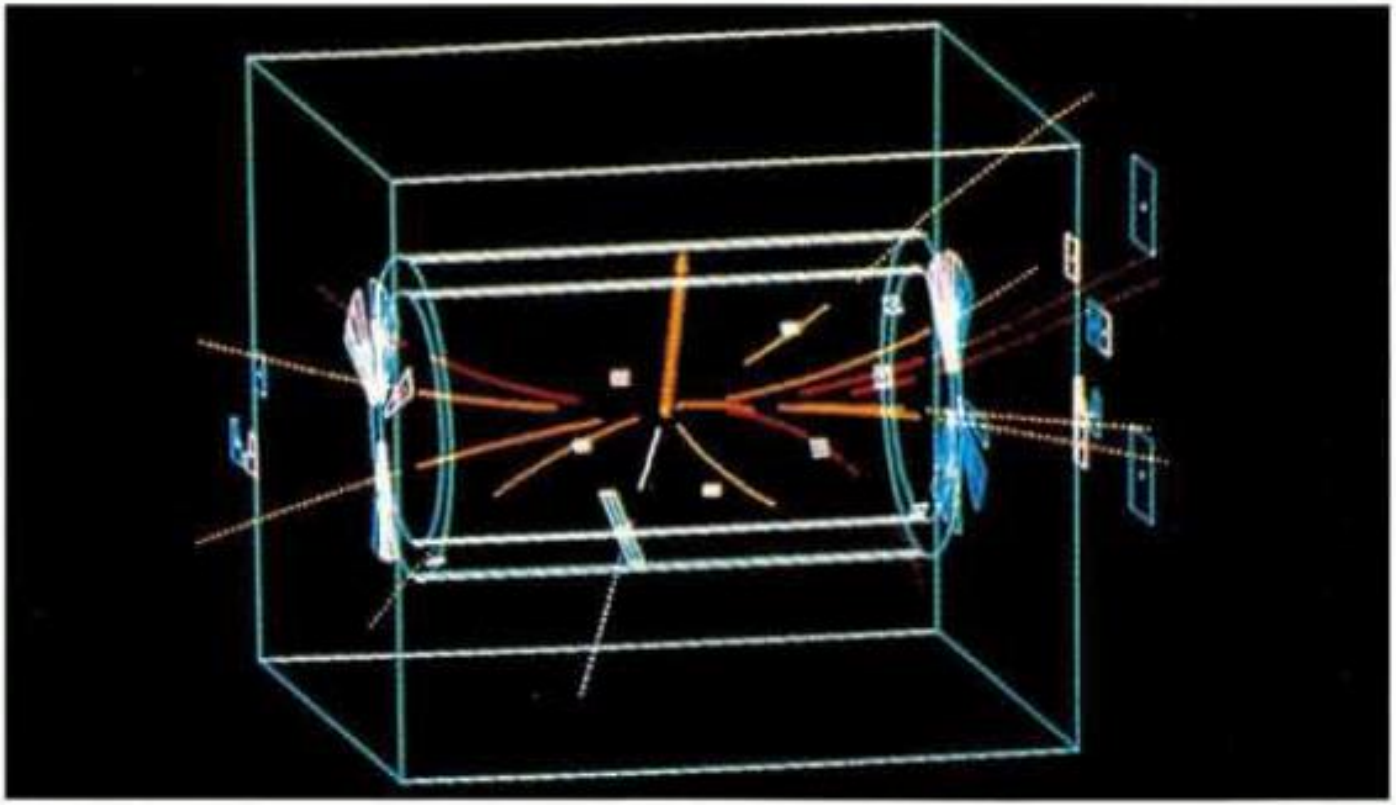

The decay of a W particle in the UA1 detector, showing the track of the high-energy electron towards the bottom. The yellow arrow marks the direction of the missing transverse energy and hence the path of the unseen neutrino.

CERN Courier 2003 num. 4

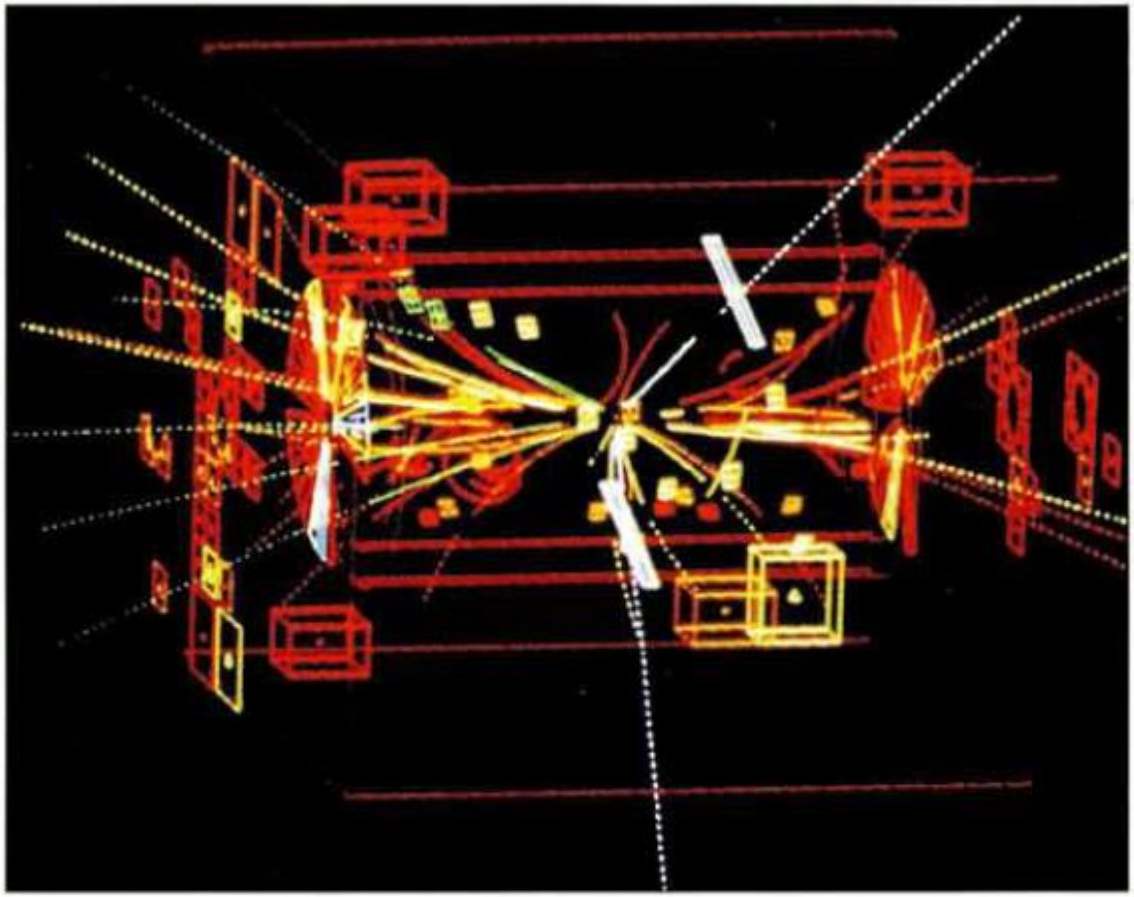

One of the first Z particles observed in UA1. The two white tracks (towards the top right and almost directly downwards) reveal the Z's decay into an electron–positron pair that deposit their energy in the electromagnetic calorimeter.

CERN Courier 2003 num. 4

CERN SPS 1982-1991, UA1, UA2 results

Observation of W and Z

Production cross sections, decay channels

Masses, widths, branching ratios

Lepton universality

Differential distributions

Standard Model parameters

LEP, CERN 1989 – 2000

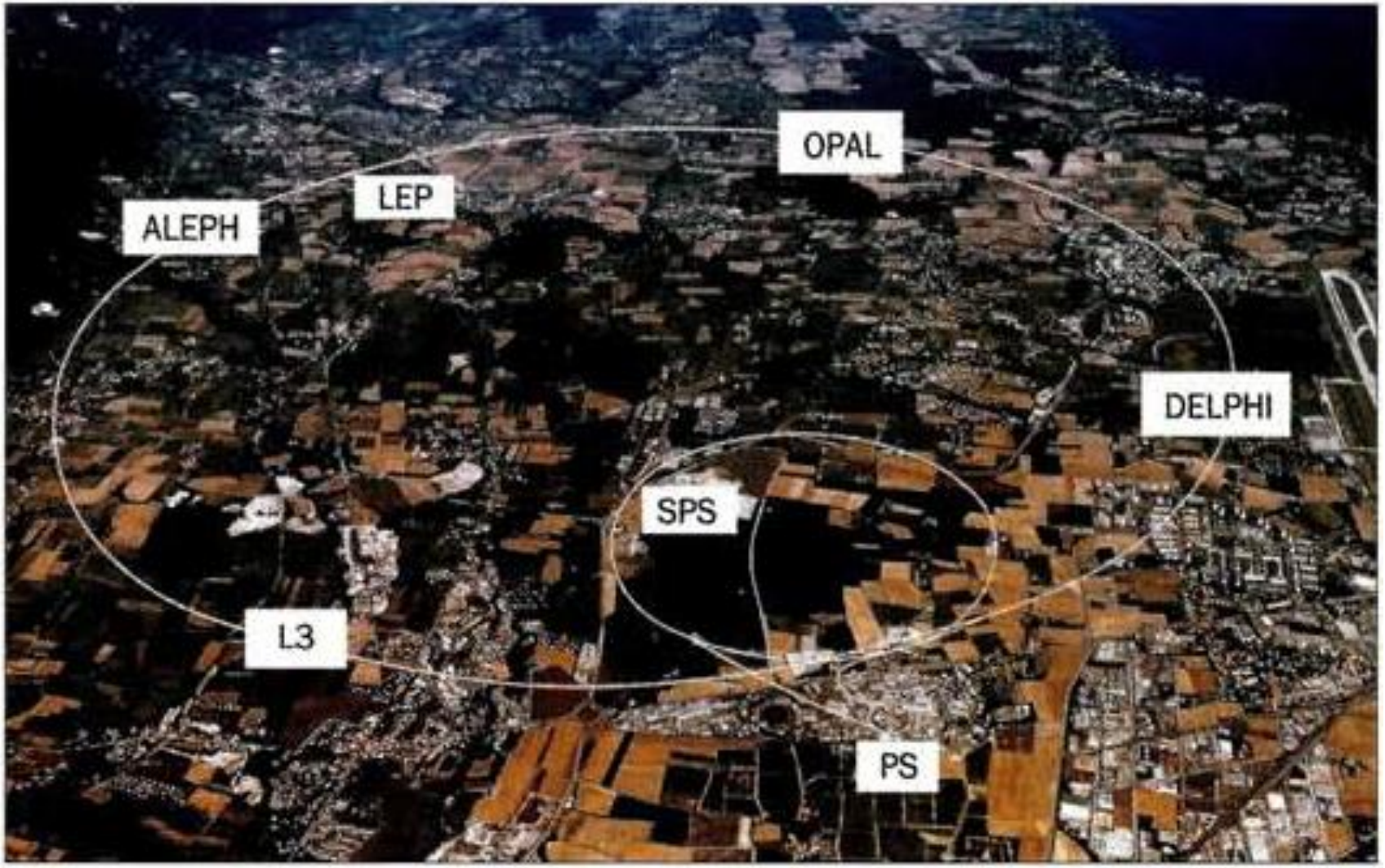

CERN Courier 2004 num. 4

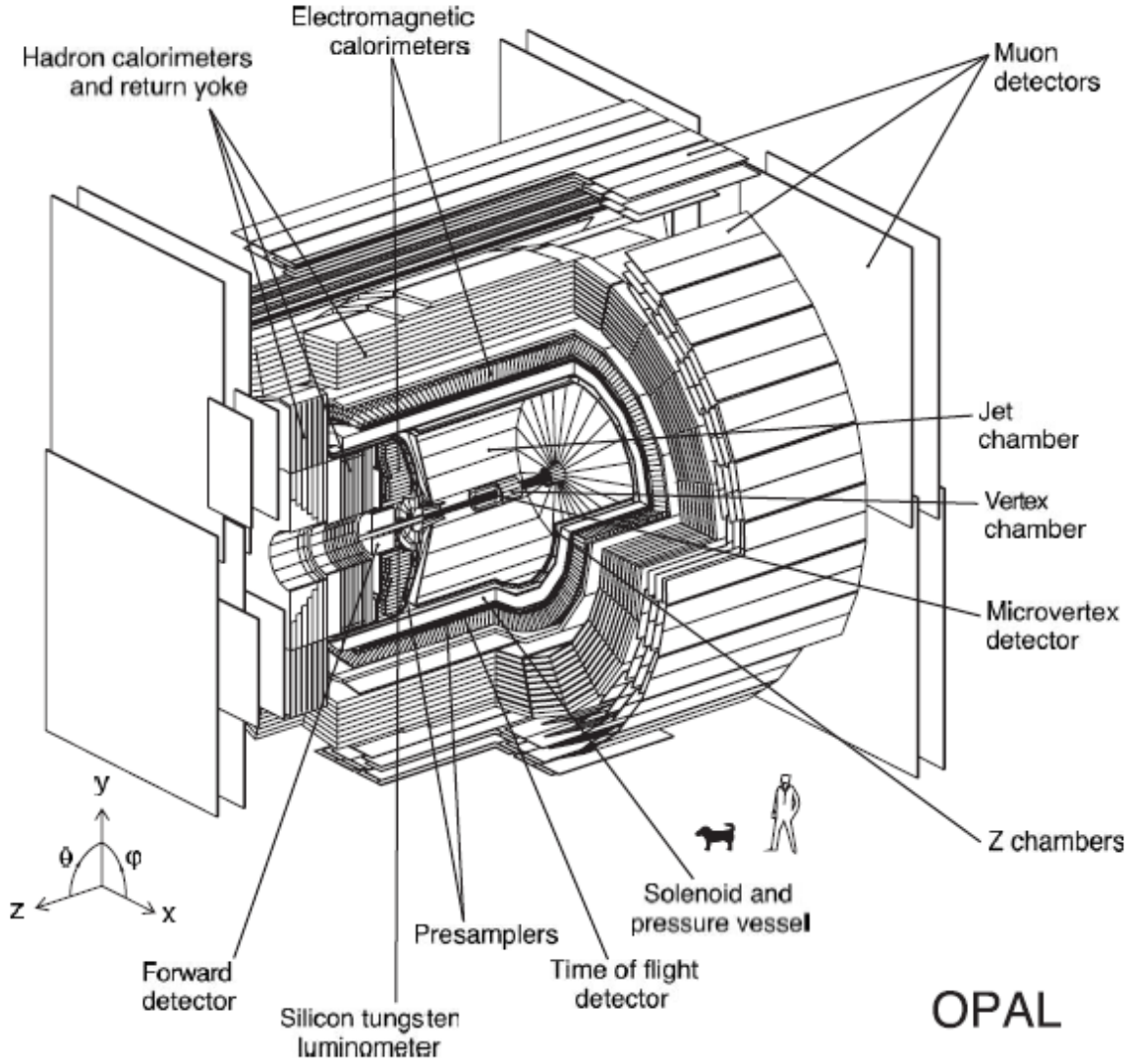

Fig. 1.6. A cut-away view of the OPAL detector, as an example LEP/SLC detector. The z-axis points along the direction of the electron beam.

Physics Reports 427 (2006) 257 – 454 p. 266

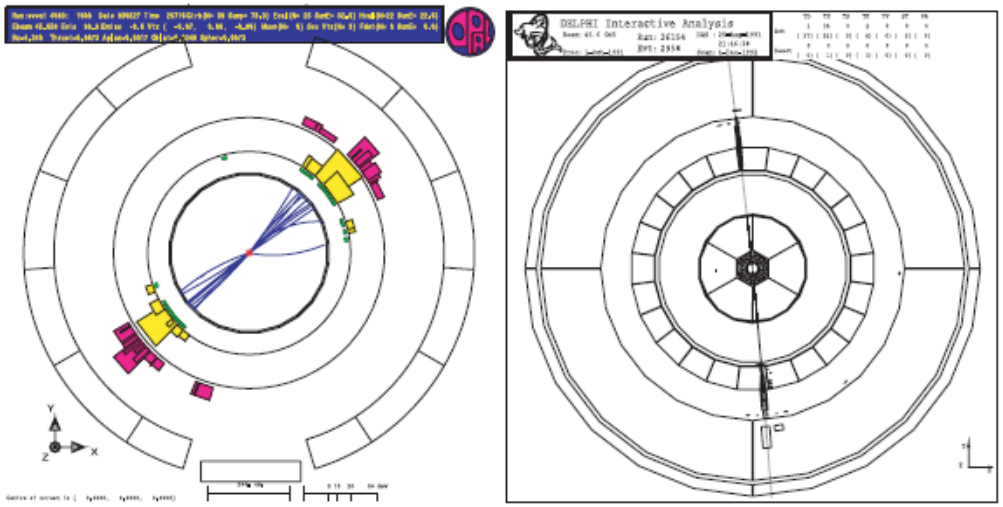

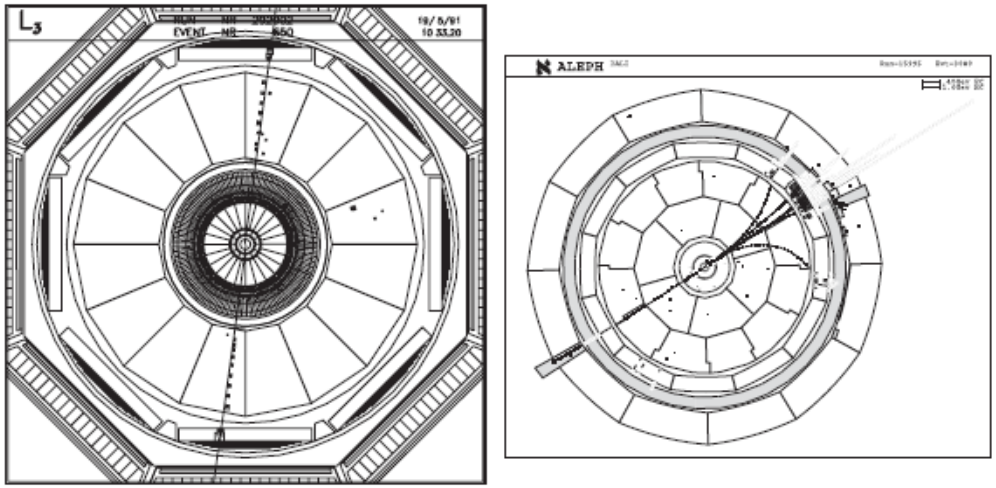

OPAL

$$Z \to q\bar{q}$$

DELPHI

$$Z \to e^+e^-$$

L3

$$Z \to \mu^+\mu^-$$

ALEPH

$$Z \to \tau^+\tau^-$$

Fig. 1.7. Pictures of $q\bar{q}$, e^+e^-, $\mu^+\mu^-$ and $\tau^+\tau^-$ final states, visualised with the event displays of the OPAL, DELPHI, L3 and ALEPH collaborations, respectively. In all views, the electron–positron beam axis is perpendicular to the plane of the page. The stability of the electron and the long lifetime of the muon allow these fundamental Z decays to be directly observed, while the low-multiplicity products of τ decays are confined to well-isolated cones. Hadronic Z decays result in higher-multiplicity jets of particles produced in the QCD cascades initiated by the initial $q\bar{q}$ pair.

Physics Reports 427 (2006) 257 – 454 p. 267

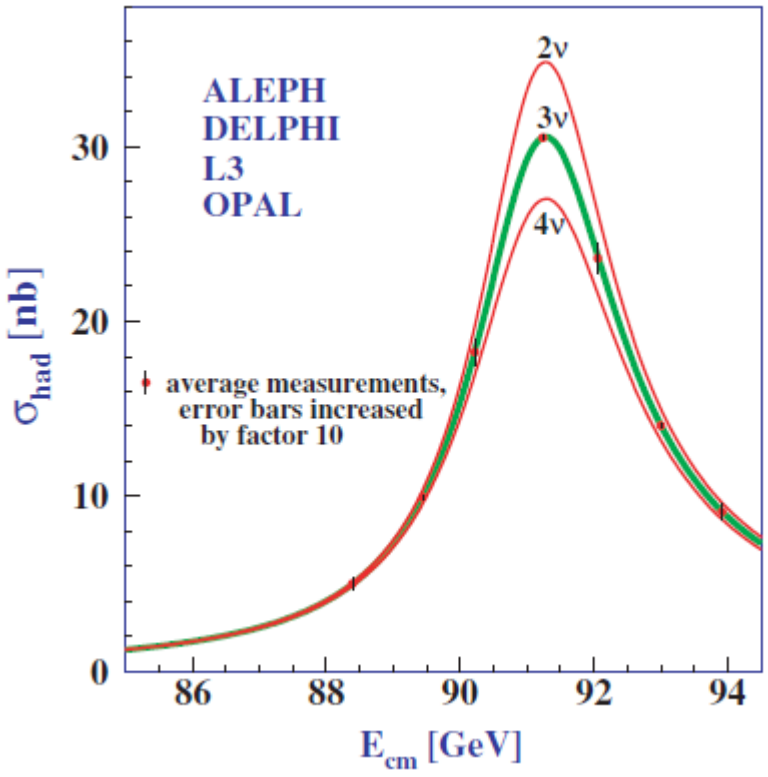

"Precision electroweak measurements on the Z resonance"

LEP Run 1 : 1989 – 1995

CMS energy 91 GeV
each experiment collected
4.5 millions of Z decays
17 millions altogether

SLC : 1992 – 1998
experiment **SLD** collected
600 000 of Z decays with
polarised beams
precision tagging of c and
b decays of Z

LEP Run 2 : 1996 – 2000

CMS energy 161 - 209 GeV

Physics Reports 427 (2006) 257 – 454

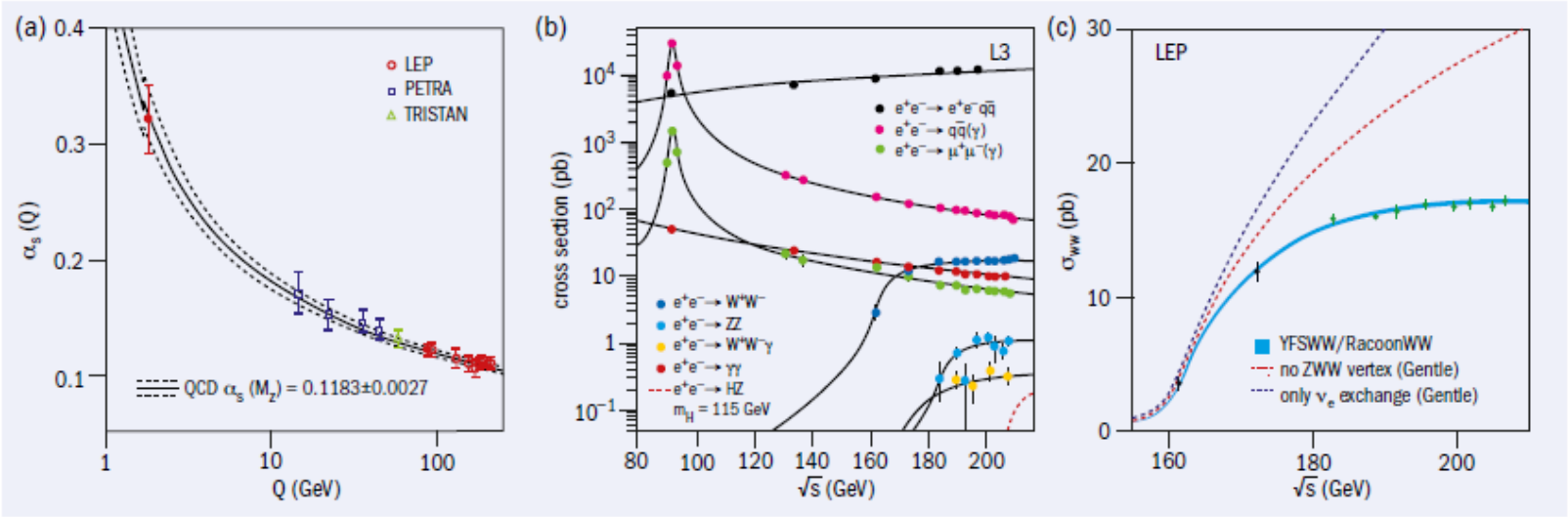

Fig. 2. *(a) The running of the strong coupling constant, measured both at LEP and in deep-inelastic-scattering experiments, as a function of the energy scale, as predicted by QCD. (b) The LEP physics landscape, starting at the Z peak, above which the cross section is dominated by two-photon reactions ($e^+e^- \to e^+e^- q\bar{q}$). Other cross sections fall rapidly. The W and Z pair cross-sections become visible at 160 and 182 GeV. No Higgs boson was seen at LEP, excluding the mass range from 15 MeV to 115 GeV. (c) The LEP ring was designed to test the cancellation of the various diagrams for WW production that arise in the electroweak gauge theory. In the absence of electroweak unification, only the neutrino exchange diagram would be present, and the cross section would diverge.*

LEP II: 1996 – 2000, 161 – 209 GeV

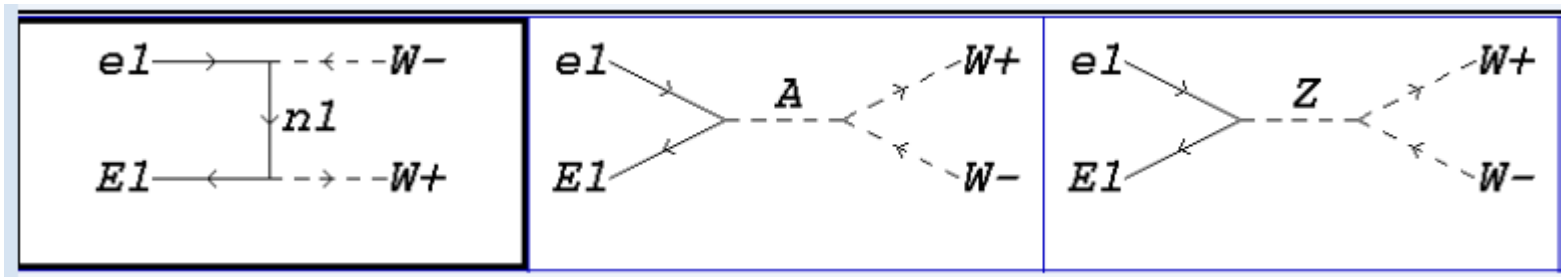

CERN Courier 2019, num. 5

Tevatron

Fermilab 1987 – 2011 1.8 – 1.96 TeV

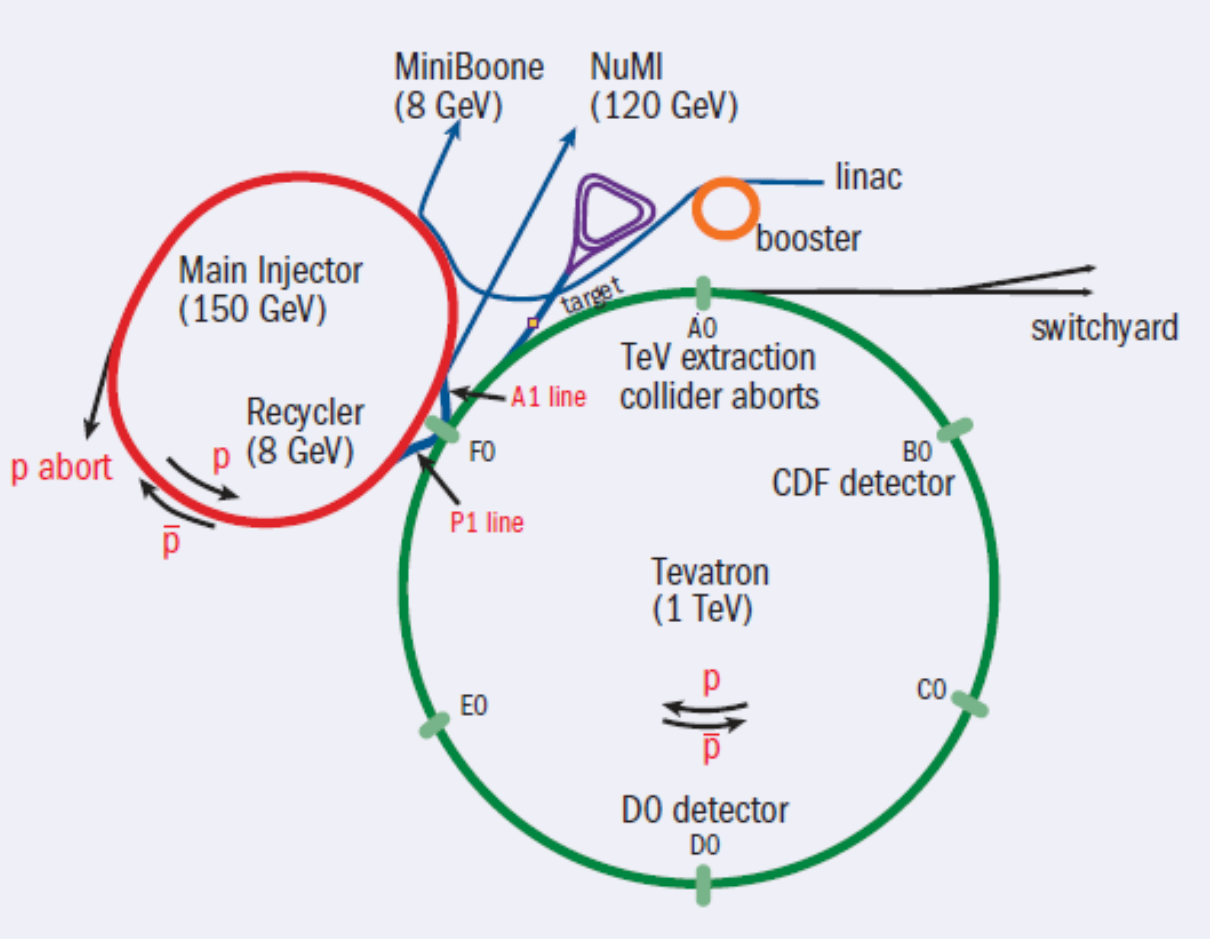

The Fermilab accelerator complex during Tevatron Run II.

CERN Courier 2011 num. 9

D0, CDF

Run 1: 1992 – 1996 1.8 TeV

Run 2: 2001 – 2011 1.96 TeV luminosity x 10

Each experiment collected 10 inverse fb with 5 millions W and 400 000 Z.

Results from Tevatron

- **W boson mass** and width
- Z boson mass and width
- FB assymetry in Z decays
- Lepton charge assymetry in W decays
- W and Z boson production total and differential cross sections
- W+jets and Z+jets cross sections, cross sections ratios
- Diboson production WW, WZ, ZZ, Wgamma*, Zgamma*
- Limits on aTGC and aQGC

LHC
Large Hadron Collider

- LHC is a proton-proton collider. It is situated in the tunnel of former electron-positron collider LEP.
- Project was born in 1984, it was approved in 1995 and the construction started in 1999.
- LHC is working from 2009. During the Run 1 in the years 2009-2012 it took data at the energy 7 and 8 TeV.
- Run 2 with CMS energy 13 TeV took place in the period 2015 - 2018. The integrated luminosity is 139 fb.
- Run 3 started this year at the energy 13.6 TeV and it will last until the end of year 2025. Planned integrated luminosity is 300 fbi.
- HL-LHC will run from 1929 until 2040 with several shutdowns. Planned integrated luminosity is 3000 fbi.

Overall view of the LHC experiments.

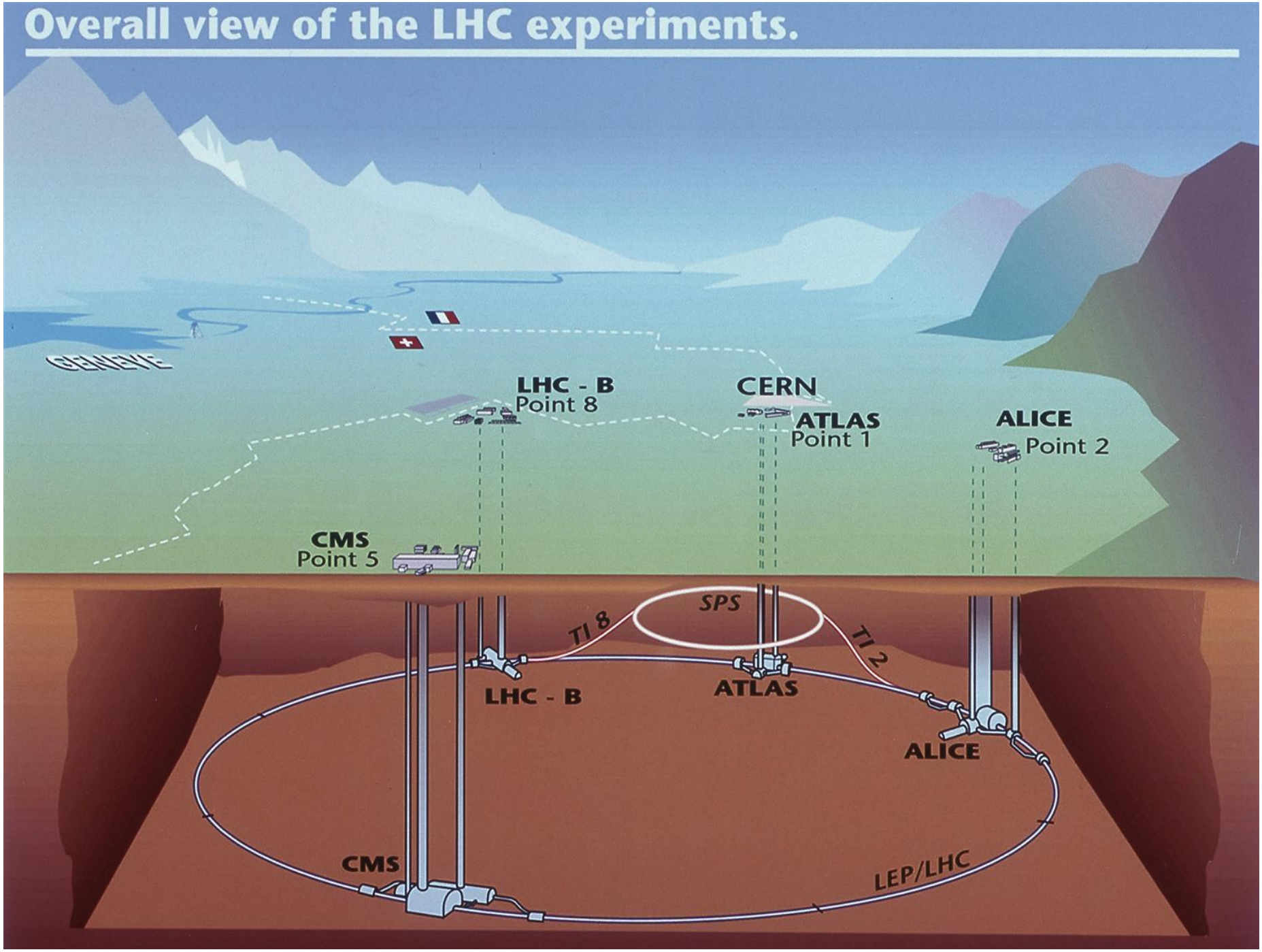

ATLAS detector

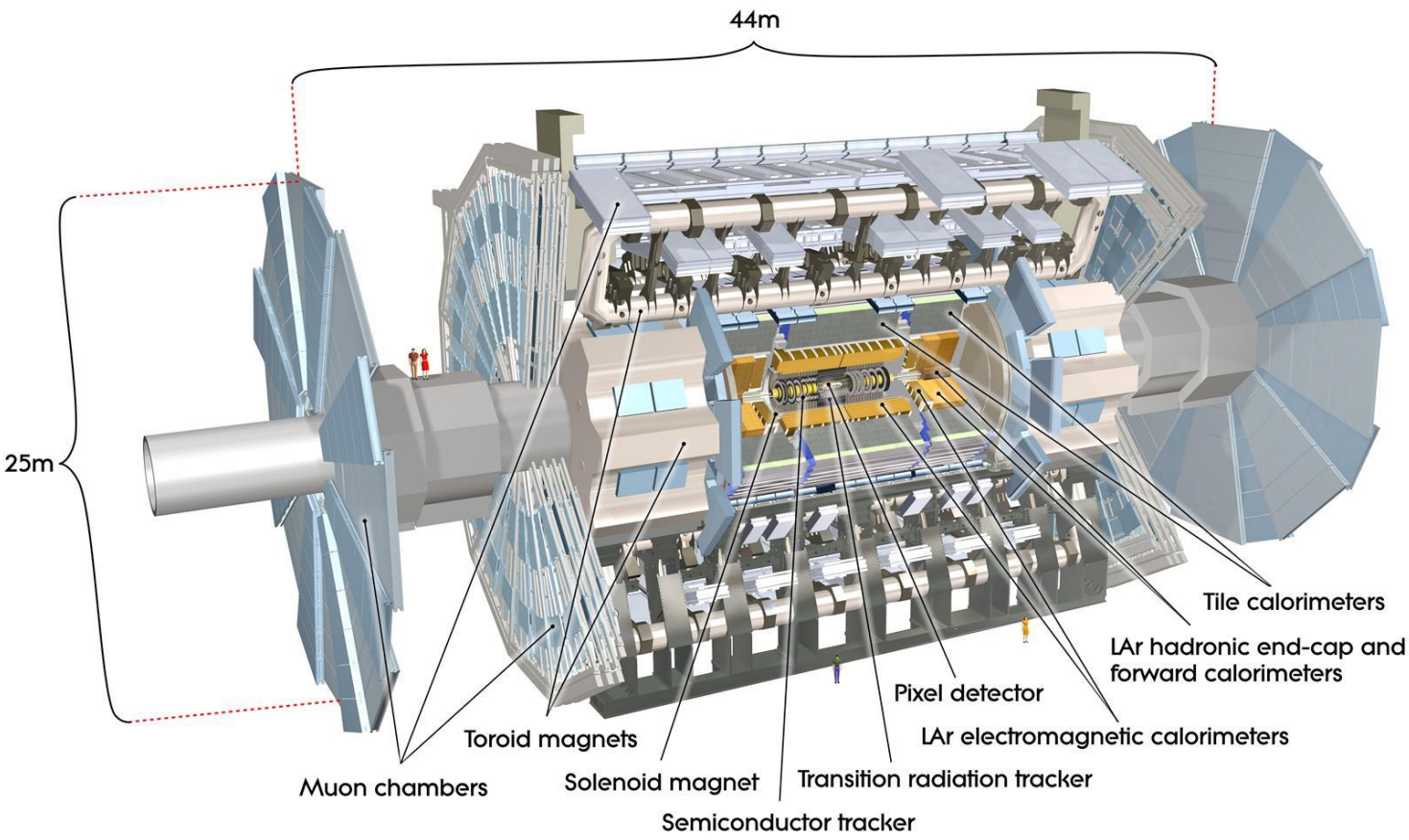

W/Z and EW measurements at **ATLAS**

More than 120 publications dealing with W and Z in total.
Wide range of topics is covered:

1) W mass, sin^2(theta_W)

2) Production cross sections of W/Z , W/Z + jets, W/Z + heavy flavours, ratios of cross sections.

3) W/Z differential distributions (Pt, rapidity, angular, ...)

4) W/Z polarisation

5) W charge asymmetry, Z FB asymmetry

6) Rich set of measurement of multiboson production

W/Z and EW measurements at **ATLAS**

Recent analyses selected for this presentation:

- W/Z cross sections at 7 TeV using the full 2011 dataset

- W mass at 7 TeV using the full 2011 dataset

- WWW production using the full Run 3 dataset

ATLAS Collaboration: Eur. Phys. J. C (2017) 77:367
2011 7 TeV $\int Ldt = 4.6\ fb^{-1}$

Precision measurement and interpretation of inclusive W^+, W^- and Z production cross sections with the ATLAS detector

1) Inclusive cross sections
2) Test of lepton universality
3) Differential cross sections
4) Interpretation of data in NNLO QCD analysis
5) Ratio of strange-to-light sea quarks densities determined
6) New measurement of the CKM matrix element |Vcs|

Measurements are performed in electron and muon channels and finally they are combined.

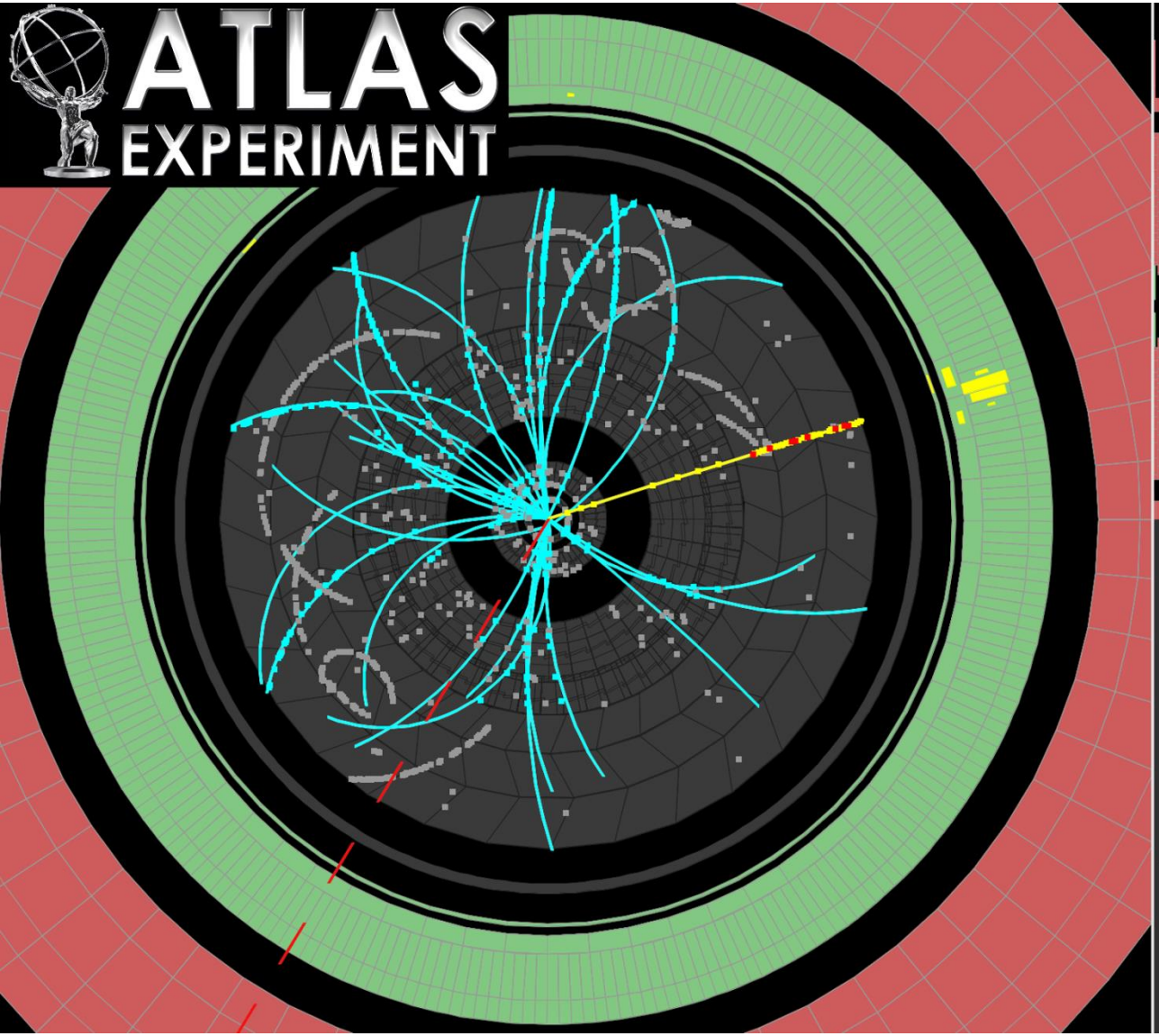
ATLAS
EXPERIMENT

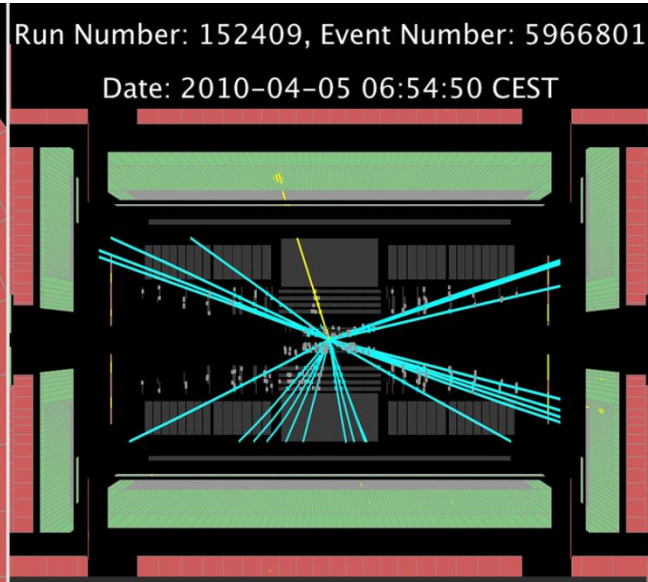
Run Number: 152409, Event Number: 5966801
Date: 2010-04-05 06:54:50 CEST

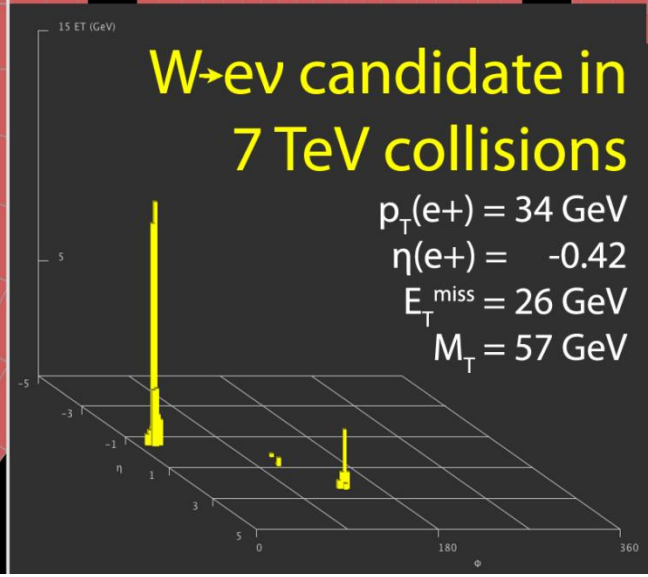
15 ET (GeV)
W→eν candidate in
7 TeV collisions
p_T(e+) = 34 GeV
η(e+) = -0.42
E_T^{miss} = 26 GeV
M_T = 57 GeV
5
-5
-3
-1
η
1
3
5
0
180
360
Φ

ATLAS Collaboration: Eur. Phys. J. C (2017) 77:367
2011 7 TeV $\int Ldt = 4.6\ fb^{-1}$

Fiducial phase space definitions

$$l = e, \mu$$

$W^{\pm} \to l^{\pm}\nu$: $P_{T,l} > 25\ GeV, |\eta_l| < 2.5,\ P_{T,\nu} > 25\ GeV, m_T > 40\ GeV$

Central $Z \to ll$: $P_{T,l} > 20\ GeV, |\eta_l| < 2.5,\ 46\ GeV < m_{ll} < 150\ GeV$

Forward $Z \to ll$: $P_{T,l} > 20\ GeV, |\eta_{l_1}| < 2.5, 2.5 < |\eta_{l_2}| < 4.9$

$66\ GeV < m_{ll} < 150\ GeV$

Theoretical predictions:
QCD NNLO : DYNNLO 1.5, FEWZ 3.1.b2
EW NLO: MCSANC 1.20
PDF: ATLAS-epWZ12

ATLAS Collaboration: Eur. Phys. J. C (2017) 77:367
2011 7 TeV $\int Ldt = 4.6\ fb^{-1}$

Improved precision

0.6%, 0.5% and 0.32%, precision reached for W^+, W^- and Z, respectively, appart of the common 1.8% normalization uncertainty due to the luminosity specification. The differential measurements are nearly as precise except the edges of the phase space.

	$\sigma^{tot}_{W\to\ell\nu}$ [pb]
$W^+ \to \ell^+\nu$	$6350 \pm 2\,(stat) \pm 30\,(syst) \pm 110\,(lumi) \pm 100\,(acc)$
$W^- \to \ell^-\bar{\nu}$	$4376 \pm 2\,(stat) \pm 25\,(syst) \pm 79\,(lumi) \pm 90\,(acc)$
$W \to \ell\nu$	$10720 \pm 3\,(stat) \pm 60\,(syst) \pm 190\,(lumi) \pm 130\,(acc)$
	$\sigma^{tot}_{Z/\gamma^*\to\ell\ell}$ [pb]
$Z/\gamma^* \to \ell\ell$	$990 \pm 1\,(stat) \pm 3\,(syst) \pm 18\,(lumi) \pm 15\,(acc)$

ATLAS Collaboration: Eur. Phys. J. C (2019) 79:901

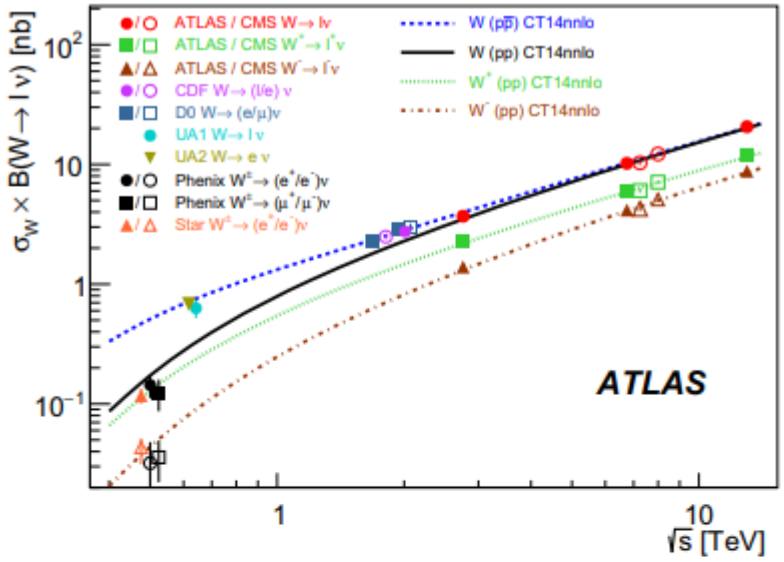

(a)

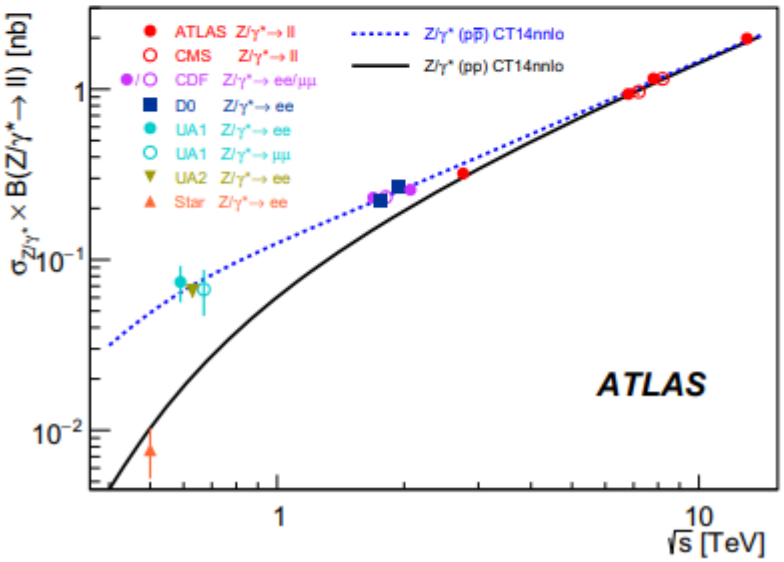

(b)

ATLAS Collaboration: Eur. Phys. J. C (2017) 77:367
2011 7 TeV $\int Ldt = 4.6\ fb^{-1}$

Test of electron-muon universality

Many systematic uncertainties cancel in the ratio.

$$R_W = \frac{\sigma^{fid}_{W\to e\nu}}{\sigma^{fid}_{W\to \mu\nu}} = \frac{BR(W\to e\nu)}{BR(W\to \mu\nu)} = 0.9967 \pm 0.0004(stat) \pm 0.0101(syst)$$

This measurement is more precise than the combination of **LEP** results, **CDF** and **LHCb Collaboration**. It also significantly improves the previous **ATLAS** measurement.

$$R_Z = \frac{\sigma^{fid}_{Z\to ee}}{\sigma^{fid}_{Z\to \mu\mu}} = \frac{BR(W\to ee)}{BR(W\to \mu\mu)} = 1.0026 \pm 0.0013(stat) \pm 0.0048(syst)$$

This measurement is in agreement with the combined result of **LEP** and **SLC** data and again, significantly more precise than the **ATLAS** measurements with the 2010 and 2015 data.

ATLAS Collaboration: Eur. Phys. J. C (2017) 77:367
2011 7 TeV $\int Ldt = 4.6\ fb^{-1}$

The orange and blue bands correspond to the measurements for on-shell **W** and **Z** production as obtained at **LEP** and **SLC**. The **SM** expectation is indicated with an open circle.

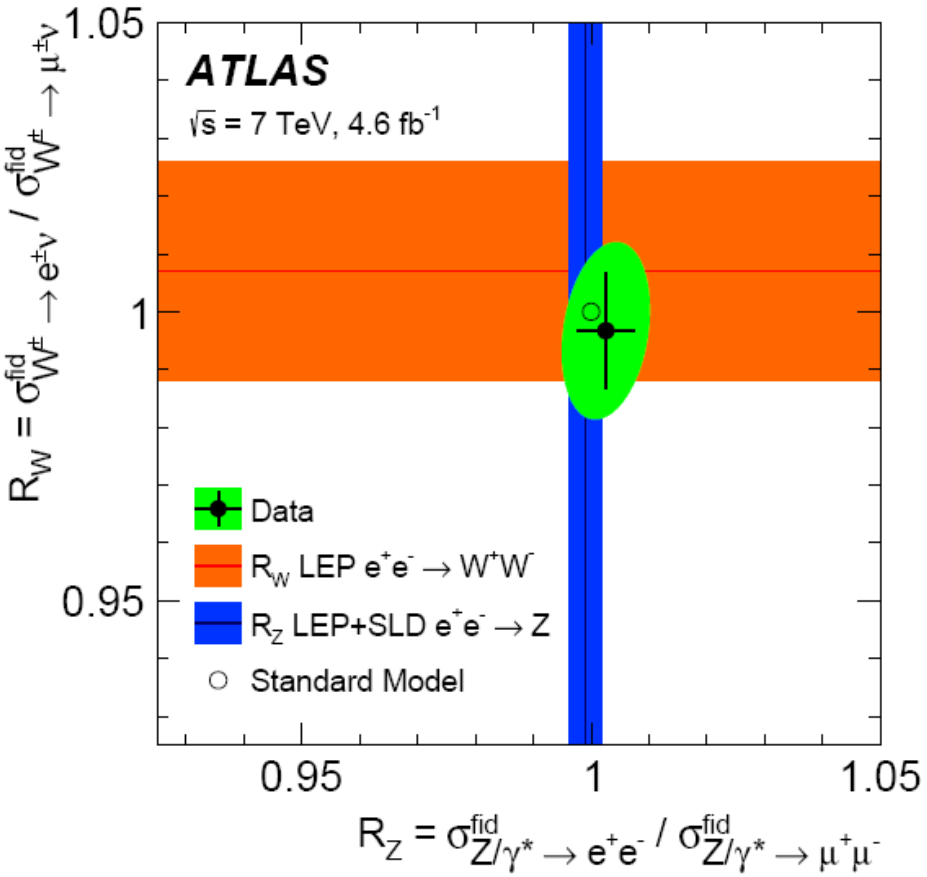

ATLAS Collaboration: Eur. Phys. J. C (2017) 77:367
2011 7 TeV $\int Ldt = 4.6\ fb^{-1}$

Fiducial cross sections discriminate between PDFs

NNLO QCD predictions with **NLO EW** corrections based on the **ABM12**, **CT14**, **HERAPDF2.0**, **JR14**, **MMHT2014** and **NNPDF3.0** PDF sets are compared to the data. PDF sets **CT14**, **MMHT2014** and **NNPDF3.0** give predictions that are lower both for the **W** positive and the **W** negative, and the same trend is observed also for **Z**.

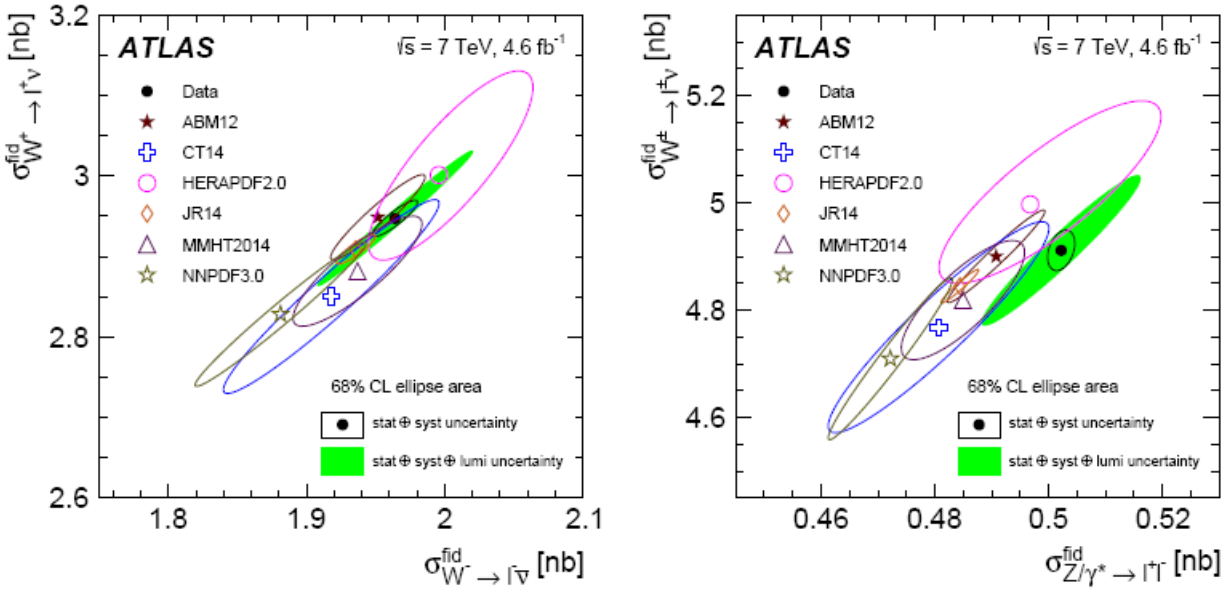

ATLAS Collaboration: Eur. Phys. J. C (2017) 77:367
2011 7 TeV $\int Ldt = 4.6\ fb^{-1}$

Cross section ratios

The measured **W** positive / **W** negative ratio is well reproduced, but all PDF sets predict a higher **W/Z** ratio than measured in the data.

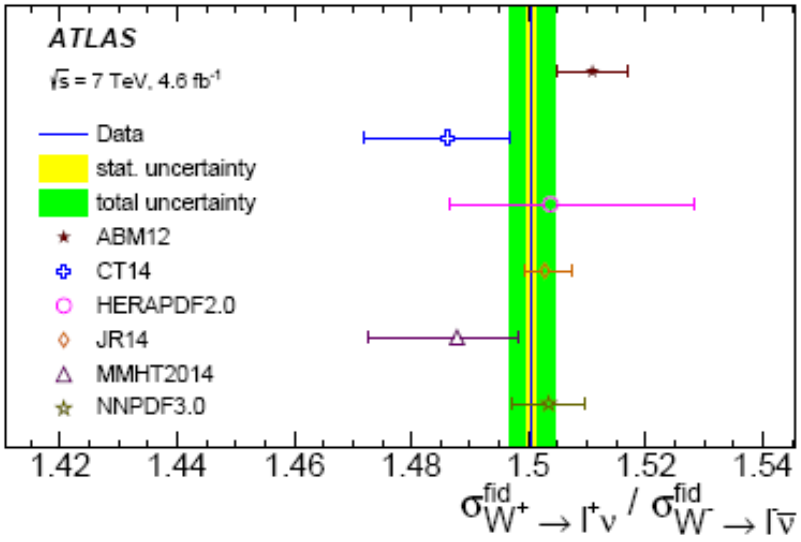

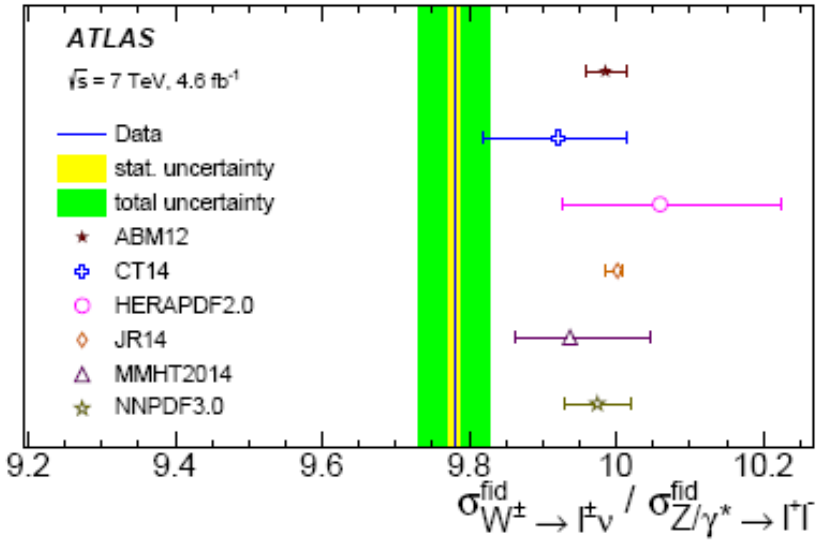

ATLAS Collaboration: Eur. Phys. J. C (2017) 77:367
2011 7 TeV $\int Ldt = 4.6\ fb^{-1}$

Differential distributions

The predictions with the **ABM12** PDF set match data particularly well, while the predictions of **NNPDF3.0**, **CT14**, **MMHT14** and **JR14** tend to be below and the **HERAPDF2.0** set slightly above the **W** cross section data.

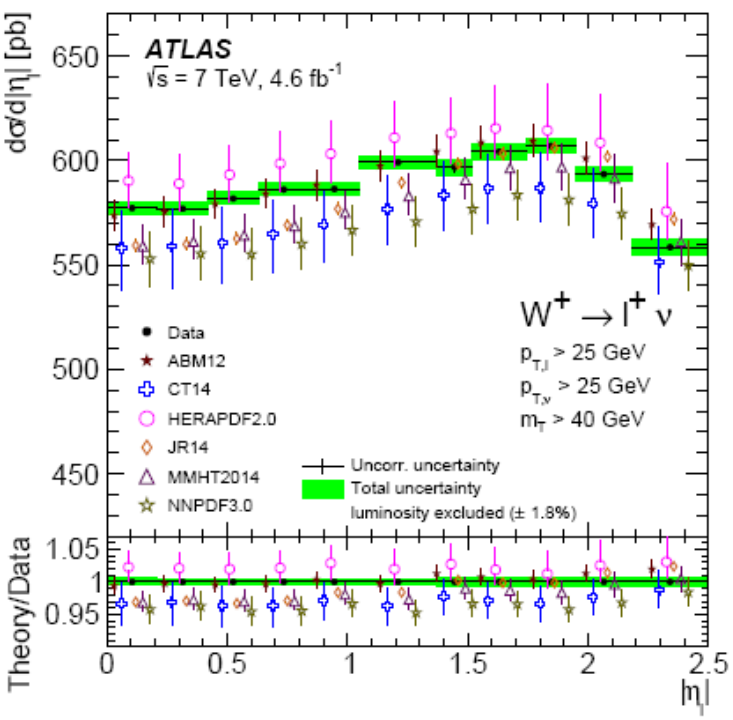

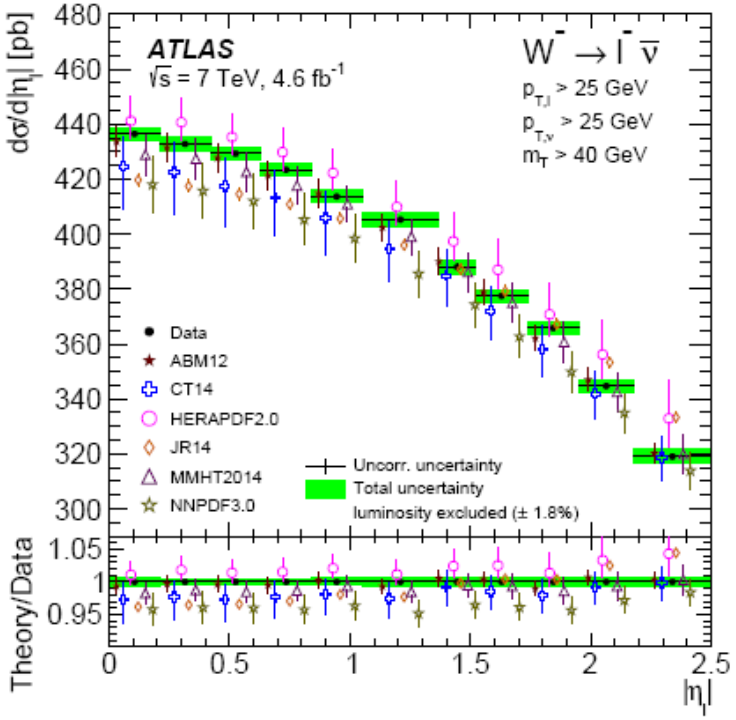

ATLAS Collaboration: Eur. Phys. J. C (2017) 77:367

2011 7 TeV $\int Ldt = 4.6\ fb^{-1}$

QCD analysis

Differential **Drell-Yan** production cross-sections are studied in combination with the final **NC** and **CC DIS HERA** I+II data within the framework of perturbative QCD. New set of PDFs obtained: **ATLAS-epWZ16**

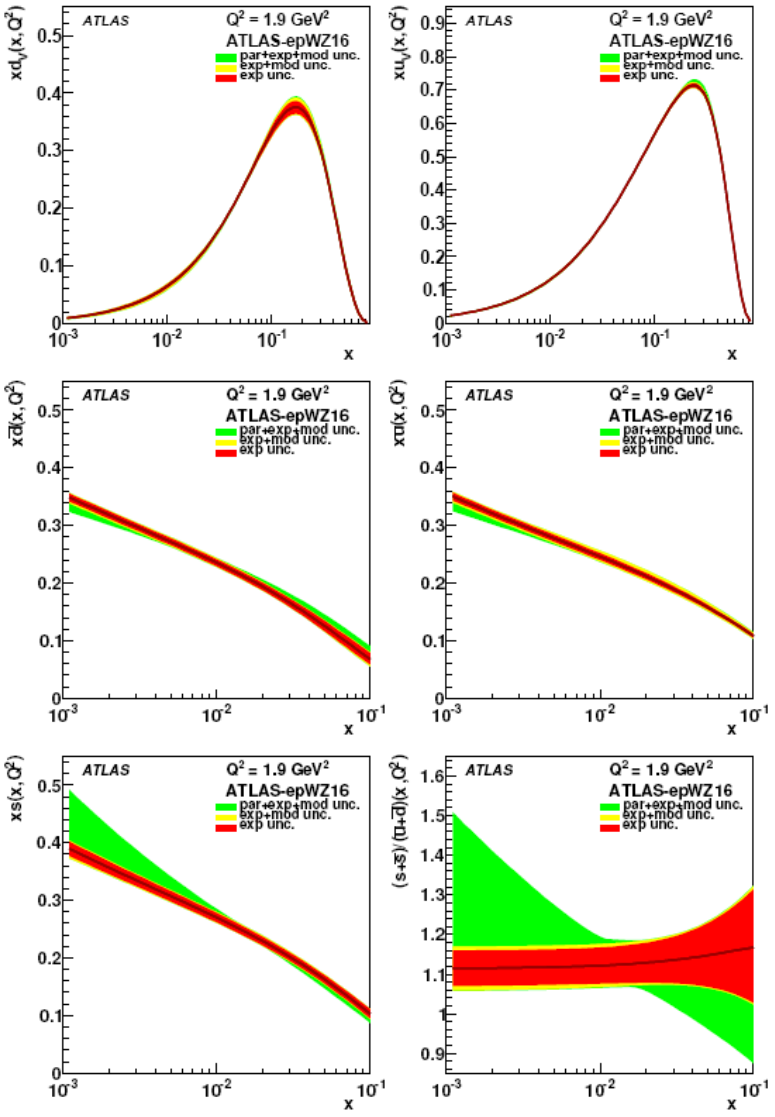

ATLAS Collaboration: Eur. Phys. J. C (2017) 77:367
2011 7 TeV $\int Ldt = 4.6\ fb^{-1}$

Strangeness enhancement

Recent global fit analyses **ABM12**, **MMHT14**, **CT14** and **NNPDF3.0** predict both ratios to be significantly lower than unity, with values between 0.4 and 0.6. ATLAS data sees enhanced strangeness.

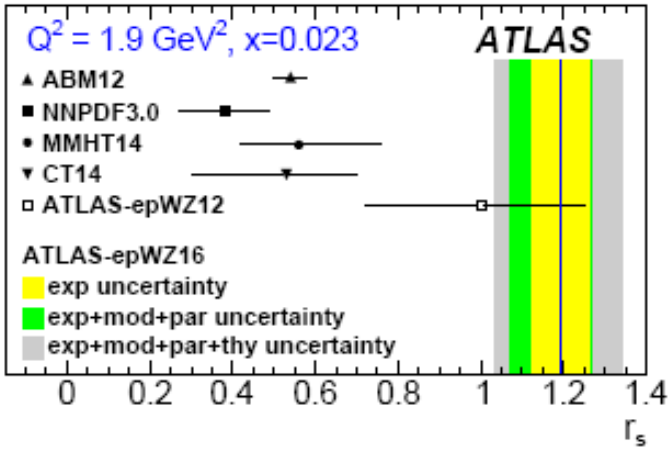

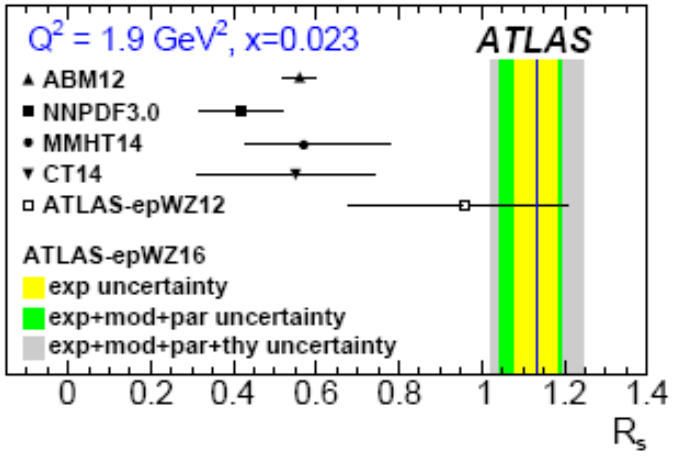

$$r_s = \frac{s + \bar{s}}{2\bar{d}}$$

$$R_s = \frac{s + \bar{s}}{\bar{u} + \bar{d}}$$

ATLAS Collaboration: Eur. Phys. J. C (2017) 77:367
2011 7 TeV $\int Ldt = 4.6\ fb^{-1}$

Competitive determination of the value of $|V_{cs}|$

ATLAS specification is compared with the determinations obtained from the leptonic Ds decay and semileptonic D meson decay obtained from data of **CLEO-c**, **BABAR** and **Belle Collaboration**. In addition, an early determination by the **NNPDF Collaboration** from the **QCD** fit is shown.

$$|V_{cs}| = 0.969 \pm 0.013(\text{exp})^{+0.006}_{-0.003}(\text{mod})^{+0.003}_{-0.027}(par)^{+0.011}_{-0.005}(thy)$$

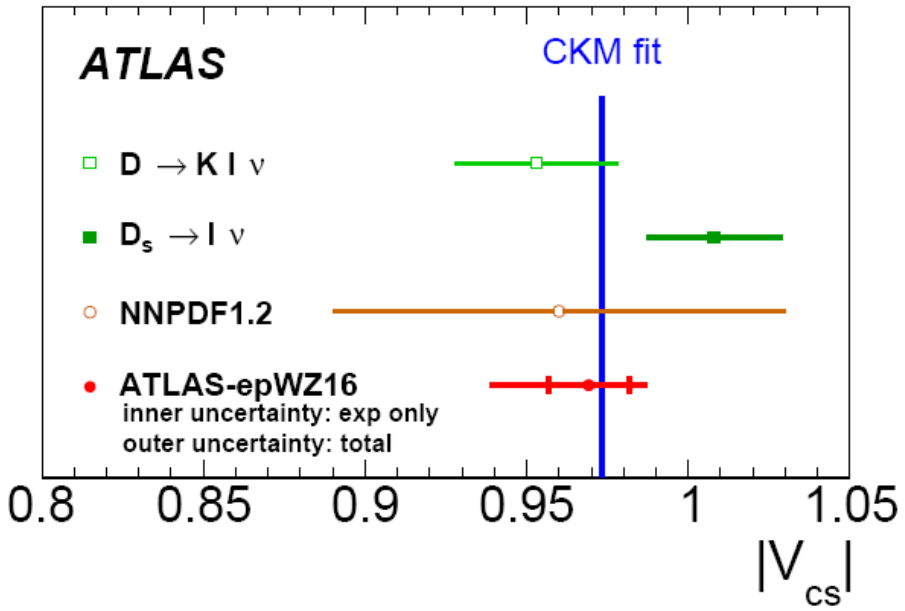

ATLAS Collaboration: Eur. Phys. J. C (2018) 78:110
2011 7 TeV $\int Ldt = 4.6\ fb^{-1}$

Measurement of the W-boson mass in pp collisions at $\sqrt{s} = 7$ TeV with the ATLAS detector

This measurement is very interesting from the point of view of new physics.

The W mass is a unique prediction of standard model. At the tree level, its value is determined by the values of weak mixing angle and mass of Z boson.

Gauge couplings and masses of other SM particles, especially those of top quark and Higgs boson, enters into higher order corrections. Existence of new particles and new interactions might modify W mass value, thus providing signal of new physics.

ATLAS Collaboration: Eur. Phys. J. C (2018) 78:110
2011 7 TeV $\int Ldt = 4.6\ fb^{-1}$

The method: m_W was obtained from the fits to the transverse momentum of the charged lepton and to the transverse mass of the W boson. Templates including signal and background were simulated for several values of W boson mass. The templates were compared to the measured distributions by means of χ^2 test. The measured value of m_W is determined by the analytical minimization of the χ^2 distribution.

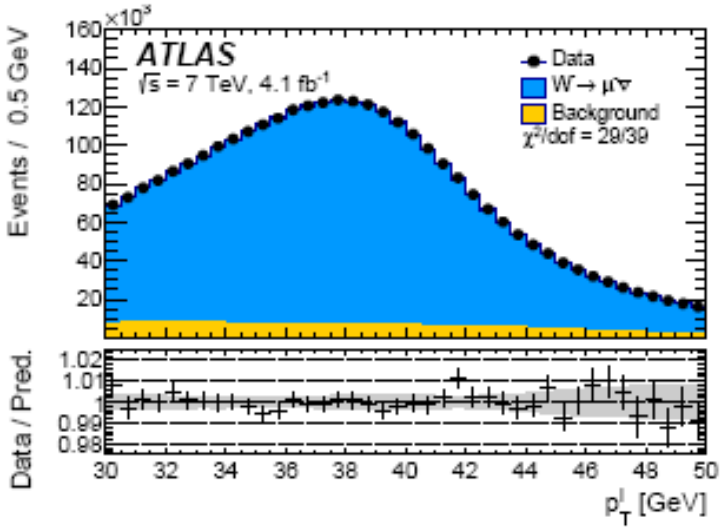

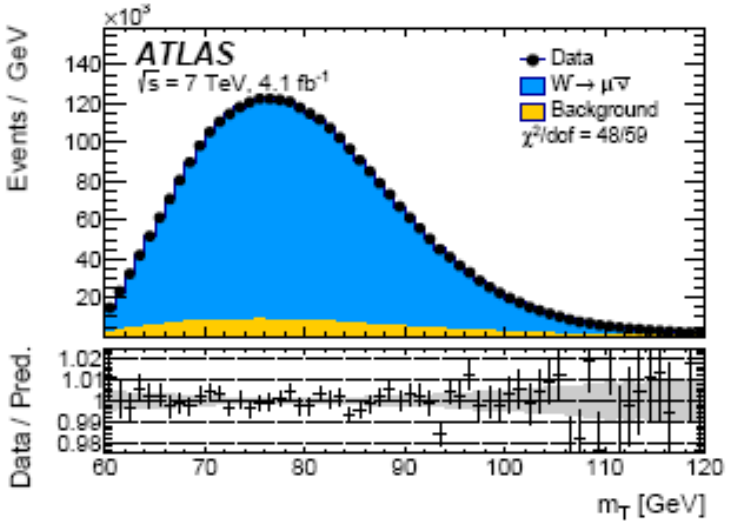

Uncertainties: dominant part of the overall uncertainty of the W mass measurement is formed by the modelling uncertainties. Especially better knowledge of the PDFs and improved predictions for the Drell-Yan production is needed for future measurement of the W-boson mass at the LHC.

ATLAS Collaboration: Eur. Phys. J. C (2018) 78:110
2011 7 TeV $\int Ldt = 4.6\ fb^{-1}$

W boson mass measurement

7.9 millions of W in muon channel, 5.9 millions in electron channel

$$m_W = 80370 \pm 7(stat) \pm 11(\exp.syst.) \pm 14(\mathrm{mod}.syst.)\ MeV$$
$$= 80370 \pm 19\ MeV$$

$$m_{W^+} - m_W = -29 \pm 28\, MeV$$

The **W**-boson mass measurement is compatible with the current world average **80377±12 MeV** and is similar in precision to the currently leading measurements performed by the **CDF** and **D0** collaborations
the measurement CDF2022 excluding

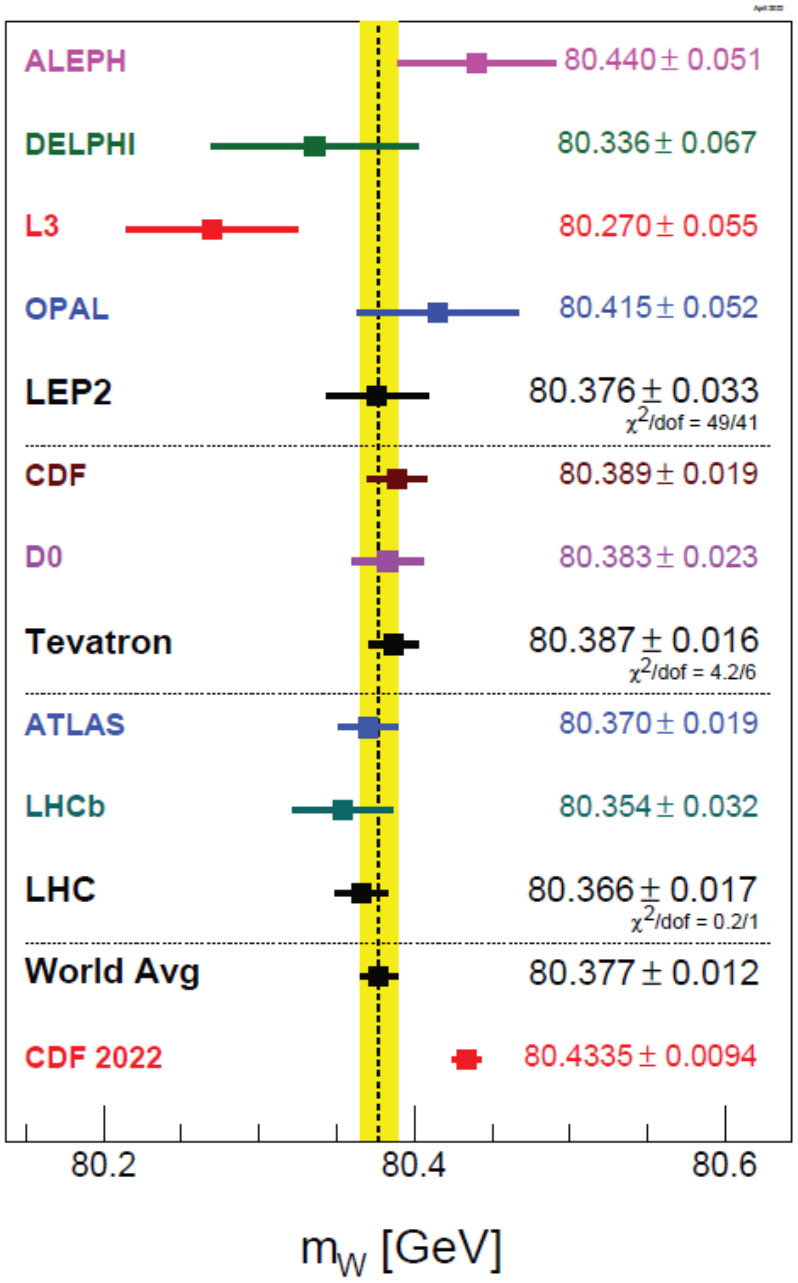

R.L. Workman *et al.* (**Particle Data Group**), **Prog. Theor. Exp. Phys. 2022, 083C01 (2022)**

CERN Courier May/June 2022

ATLAS measurement most precise from LHC measurements, similar in precision in pre-CDF 2022 Tevatron measurements

LHC challenges compared to Tevatron: non-symmetric initial state , different kinematic region => sea component c and s of PDF including more important

pileup

At higher c.m.energy, stronger dependence on modelling of p T_W spectrum

ATLAS Collaboration: PHYSICAL REVIEW LETTERS 129, 061803 (2022)

2022 13 TeV $\int Ldt = 139\ fb^{-1}$

Observation of WWW production in pp collisions at $\sqrt{s} = 13$ TeV with the ATLAS detector

The first observation of the simultaneous WWW production.
Direct probe of the strength of triple gauge coupling and quartic gauge coupling.

ATLAS Collaboration: PHYSICAL REVIEW LETTERS 129, 061803 (2022)
2022 13 TeV $\int Ldt = 139\ fb^{-1}$
CERN Courier November/December 2021

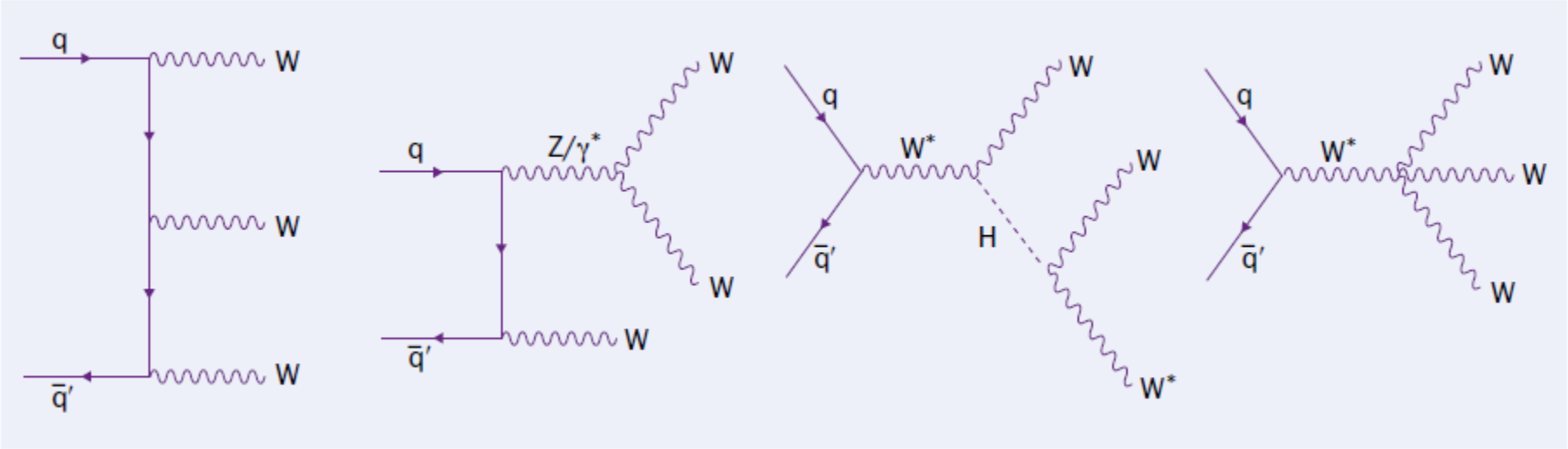

Representative LO Feynman diagrams for the production of three masive W bosons, including diagrams sensitive to triple and quartic gauge coupling

ATLAS Collaboration: PHYSICAL REVIEW LETTERS 129, 061803 (2022)
2022 13 TeV $\int Ldt = 139\ fb^{-1}$
CERN Courier November/December 2021

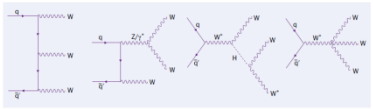

four processes at tree level
final states WWW, WWW^*

decay channels 2-lepton: $WWW \rightarrow l^{\pm}\nu l^{\pm}\nu qq$
3-lepton: $WWW \rightarrow l^{\pm}\nu l^{\pm}\nu l^{\mp}\nu$
no SFOS lepton pair
$l = e, \mu$

Dominant background : $WZ + jets$
Further background : nonprompt leptons , electrons with misidentified charge, $W\gamma/Z\gamma$ with γ misidentified as electron
SM processes with prompt leptons:
$t\bar{t}W, t\bar{t}Z, tZq, t\bar{t}H, WWZ, WZZ, ZZZ, W^{\pm}W^{\pm}jj$

ATLAS Collaboration: PHYSICAL REVIEW LETTERS 129, 061803 (2022)

2022 13 TeV $\int Ldt = 139\ fb^{-1}$

CERN Courier November/December 2021

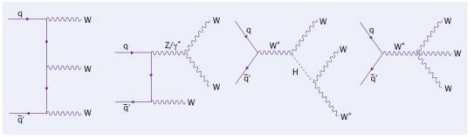

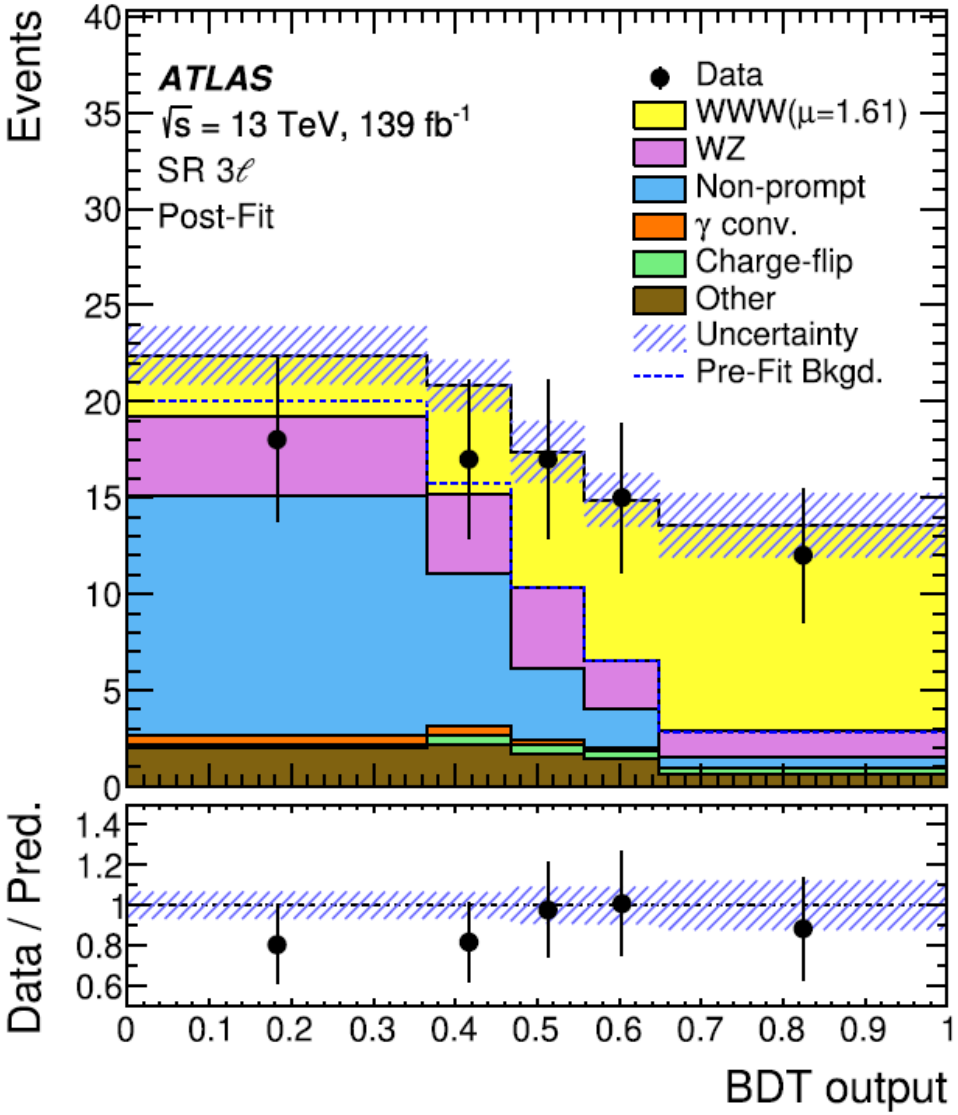

ATLAS Collaboration: PHYSICAL REVIEW LETTERS 129, 061803 (2022)
2022 13 TeV $\int Ldt = 139\ fb^{-1}$
CERN Courier November/December 2021

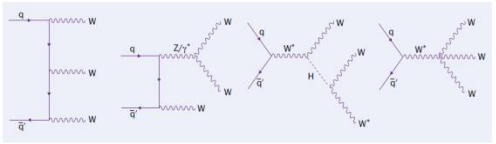

$$\sigma_{meas}(pp \to WWW) = 820 \pm 100(stat) \pm 80(syst) fb$$

$$\sigma_{predicted}(pp \to WWW) = 511 \pm 18 fb$$

NLO QCD and LO EW

Standard model background only hypothesis rejected with an observed (predicted) significance 8.0 (5.4) sigmas.

Measured cross section is 2.6 standard deviation far from the predicted one

Run 3 : expected to double available statistic

Clearifying the compatibility with SM: more precise cross section measurements, differential distributions, EFT approach

CONCLUSIONS

- Weak bosons W and Z played crucial role in the creation and establishment of electroweak and Higgs sector of Standard Model
- Bosons W and Z are present in decay chains of discovered/hypothetical particles of interest
- W and Z related measurements form essential part of physics program of all past, current and future large accelerator HEP experiments
- Established physics topics related to weak bosons:
  - testing of QCD predictions
  - constraints on PDFs
  - testing of parton emission calculations and resummation models
  - strong and stringent tests of QCD using exclusive final states
  - extraction of Standard Model parameters
  - sensitivity to the new physics
- Future: more precise tests of SM using Run 3 data and HL-LHC
- Inclusion of W/Z related data into EFT analyses